NATIONAL CENTER FOR EARTHQUAKE ENGINEERING RESEARCH

ISSN 1088-3800

Probabilistic Evaluation of Liquefaction Potential

by

H.H.M. Hwang and C.S. Lee

Technical Report NCEER-91-0025

November 25, 1991

This research was conducted at Memphis State University and was supported in whole or in part by the National Science Foundation under grant number ECE 86-07591.

NOTICE

This report was prepared by Memphis State University as a result of research sponsored by the National Center for Earthquake Engineering Research (NCEER) through a grant from the National Science Foundation, and other sponsors. Neither NCEER, associates of NCEER, its sponsors, Memphis State University nor any person acting on their behalf:

a. makes any warranty, express or implied, with respect to the use of any information, apparatus, method, or process disclosed in this report or that such use may not infringe upon privately owned rights; or

b. assumes any liabilities of whatsoever kind with respect to the use of, or the damage resulting from the use of, any information, apparatus, method, or process disclosed in this report.

Any opinions, findings, and conclusions or recommendations expressed in this publication are those of the author(s) and do not necessarily reflect the views of NCEER, the National Science Foundation, or other sponsors.

Probabilistic Evaluation of Liquefaction Potential

by

H.H.M. Hwang[1] and C.S. Lee[2]

November 25, 1991

Technical Report NCEER-91-0025

NCEER Project Numbers 89-3009 and 90-3009

NSF Master Contract Number ECE 86-07591

1 Professor, Center for Earthquake Research and Information, Memphis State University
2 Research Associate, Center for Earthquake Research and Information, Memphis State University

NATIONAL CENTER FOR EARTHQUAKE ENGINEERING RESEARCH
State University of New York at Buffalo
Red Jacket Quadrangle, Buffalo, NY 14261

PREFACE

The National Center for Earthquake Engineering Research (NCEER) is devoted to the expansion and dissemination of knowledge about earthquakes, the improvement of earthquake-resistant design, and the implementation of seismic hazard mitigation procedures to minimize loss of lives and property. The emphasis is on structures and lifelines that are found in zones of moderate to high seismicity throughout the United States.

NCEER's research is being carried out in an integrated and coordinated manner following a structured program. The current research program comprises four main areas:

- Existing and New Structures
- Secondary and Protective Systems
- Lifeline Systems
- Disaster Research and Planning

This technical report pertains to Program 1, Existing and New Structures, and more specifically to geotechnical studies.

The long term goal of research in Existing and New Structures is to develop seismic hazard mitigation procedures through rational probabilistic risk assessment for damage or collapse of structures, mainly existing buildings, in regions of moderate to high seismicity. The work relies on improved definitions of seismicity and site response, experimental and analytical evaluations of systems response, and more accurate assessment of risk factors. This technology will be incorporated in expert systems tools and improved code formats for existing and new structures. Methods of retrofit will also be developed. When this work is completed, it should be possible to characterize and quantify societal impact of seismic risk in various geographical regions and large municipalities. Toward this goal, the program has been divided into five components, as shown in the figure below:

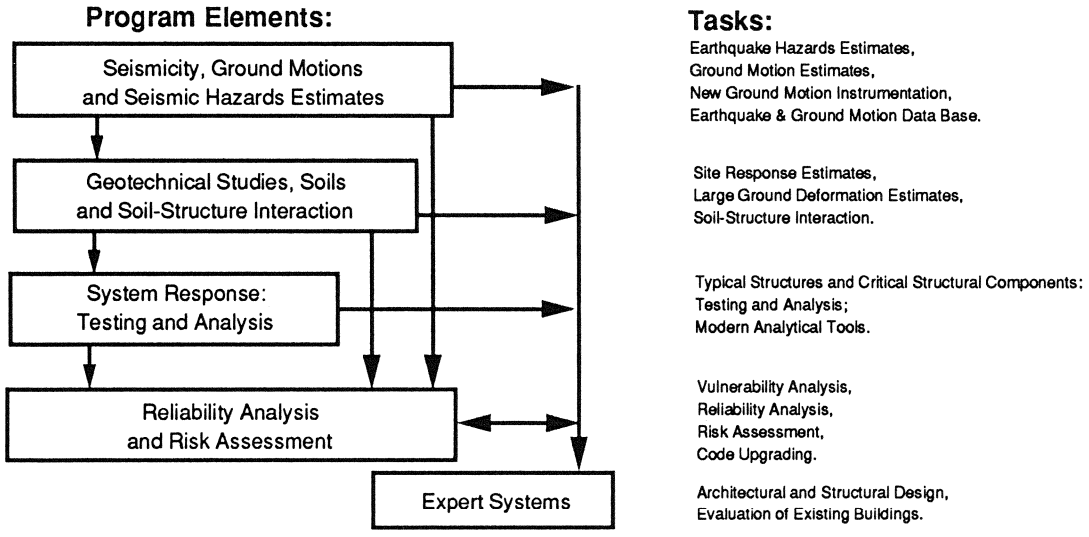

Geotechnical studies constitute one of the important areas of research in Existing and New Structures. Current research activities include the following:

1. Development of linear and nonlinear site response estimates.
2. Development of liquefaction and large ground deformation estimates.
3. Investigation of soil-structure interaction phenomena.
4. Development of computational methods.
5. Incorporation of local soil effects and soil-structure interaction into existing codes.

The ultimate goal of projects concerned with geotechnical studies is to develop methods of engineering estimation of large soil deformations, soil-structure interaction, and site response.

The purpose of this report is to develop a probabilistic method for evaluating the liquefaction potential of a saturated sand site. The method is applied to a site in Memphis, which is close to the New Madrid seismic zone. The procedure is based on an evaluation of the liquefaction potential index of a site P_L as proposed by Iwasaki. Regional seismicity and local site conditions are incorporated through relevant models. Liquefaction potential probability matrix and fragility curves are constructed by including uncertainties in the site parameters (relative density and shear modulus) as well as in various seismic parameters.

ABSTRACT

A probabilistic method for evaluating liquefaction potential of a site is presented and illustrated by using a site at President Island, Memphis, Tennessee, which is close to the New Madrid seismic zone. In this method, the liquefaction potential of a soil layer is estimated by using the factor of safety $F_L = R/L$. The earthquake-induced shear stress ratio L is determined from nonlinear site response analysis. On the other hand, the resistance shear stress ratio (or cyclic shear strength) R is determined from cyclic test data based on the equivalent uniform cycles N_{eq} and relative density D_r. The F_L value together with depth and thickness of each liquefied layer is used to calculate the liquefaction potential index of a site P_L as proposed by Iwasaki et al. (1982). The P_L value indicates the liquefaction severity of a site: no or little liquefaction ($P_L = 0$), minor liquefaction ($0 < P_L \leq 5$), moderate liquefaction ($5 < P_L \leq 15$), and major liquefaction ($P_L > 15$).

By including uncertainties in site parameters (relative density and shear modulus) and seismic parameters (stress drop, strong-motion duration, and random phase angles), 81 earthquake-site models are established. Given a moment magnitude, the probabilities of no, minor, moderate, and major liquefaction can be determined from the analyses of these earthquake-site samples. By repeating the same procedure for other moment magnitudes, the liquefaction potential probability matrix and the fragility curves can be constructed. The proposed method incorporates the local site conditions and regional seismicity in the evaluation of liquefaction potential of a site. In addition, uncertainties in seismic and site parameters can be easily included in the analysis.

ACKNOWLEDGMENTS

The assistance of Ms. Valinda Stokes in typing this manuscript is sincerely appreciated. In addition, the help provided by Ms. Tanya George and Ms. M. H. Shih in preparing the drawings is greatly acknowledged.

TABLE OF CONTENTS

LIST OF ILLUSTRATIONS

LIST OF TABLES

SECTION 1

INTRODUCTION

The catastrophic failures of structures and consequent loss of human lives due to soil liquefaction in the 1964 Niigata earthquake [1,2] have created an awareness of the danger posed by earthquake-induced liquefaction. The threat is especially imminent for sites with loose sandy soil conditions and for inadequately-compacted hydraulic fills.

The liquefaction potential of a saturated sand site is affected by site parameters such as relative density, percentage of clay, and effective confining pressure. In addition, it is also affected by seismic parameters such as the magnitude, frequency content, and duration of an earthquake. Hence, an analytical approach that incorporates the local site conditions and regional seismicity to evaluate the liquefaction potential of a site is desirable. By using the analytical method, uncertainties in seismic and site parameters can be easily included in the analysis. In this study, a probabilistic method for evaluating liquefaction potential of a site is presented and illustrated by using a site at President Island, Memphis, Tennessee, which is close to the New Madrid seismic zone (NMSZ).

The dynamic soil model for nonlinear site response analysis is established based on actual boring logs. Because of the uncertainties in relative density and shear modulus, nine site models are established. A seismologically based model that takes into account source mechanism, path attenuation, and soft-rock effects is used to generate the horizontal earthquake time

histories at the base of the soil column. The uncertainties in seismic parameters, stress drop, strong-motion duration, and random phase angles are considered in this study. From the combinations of representative values of seismic and site parameters, 81 earthquake-site samples are established for nonlinear site response analysis.

The liquefaction potential of a soil layer is estimated by using the factor of safety $F_L = R/L$. The earthquake-induced shear stress ratio L is determined from nonlinear site response analysis and is taken as the average shear stress ratio. The irregular shear stress time history for each liquefiable layer is converted into equivalent uniform cycles N_{eq} at the average shear stress ratio based on the procedure proposed by Seed et al. [3]. By using the equivalent uniform cycles N_{eq} and relative density D_r, the resistance shear stress ratio R is determined from cyclic test data. The F_L value together with depth and thickness of each liquefied layer is used to evaluate the liquefaction potential index of a site P_L proposed by Iwasaki et al. [4]. The P_L value indicates the liquefaction severity of a site: no or little liquefaction ($P_L = 0$), minor liquefaction ($0 < P_L \leq 5$), moderate liquefaction ($5 < P_L \leq 15$), and major liquefaction ($P_L > 15$).

For an earthquake with a given moment magnitude, the probabilities of no, minor, moderate, and major liquefaction can be determined from the analyses of 81 earthquake-site samples. The earthquake-induced liquefaction potential probability matrix and the fragility curves [5] can be constructed by repeating the same procedure for earthquakes with various moment magnitudes.

In this report, Section 2 describes the nonlinear site response analysis and the uncertainties in seismic and site parameters. Section 3 presents the method for evaluating the factor of safety against liquefaction for a potentially liquefiable layer and the liquefaction potential index of a site, while Section 4 presents the probabilistic method for constructing the liquefaction potential probability matrix and fragility curves. The results from the proposed method and those obtained by using the simplified approach suggested by Seed and Idriss [6,7] are compared in Section 5. Finally, Section 6 presents the conclusions of this study.

SECTION 2

NONLINEAR SITE RESPONSE ANALYSIS

It is generally acknowledged that soil liquefaction in saturated cohesionless soils during an earthquake is caused by the buildup of excess pore pressure due to the cyclic shear stress induced by ground shaking [7]. In this study, the cyclic shear stresses in a soil deposit are evaluated by performing nonlinear site response analysis using the MASH computer program [8]. The dynamic soil model in the MASH program consists of a horizontally multi-layered soil profile that extends to a fixed base. The input earthquake acceleration time histories at the base of the soil profile are synthetic earthquakes generated from a seismologically based model, in which the source mechanism, path attenuation, and soft-rock effects are taken into consideration.

2.1 Dynamic Soil Model

The existing boring log of the selected site at President Island is shown in figure 2-1. The water table of the site is about 2.5 m to 3.0 m below the ground level. Because of the capillary action of water and the silt content of the shallow soil, the top layer is considered saturated. The soil at the depth of 60 m is very stiff and thus the base of the soil profile is selected at this level. The actual bedrock (hard-rock) in the Memphis area is about 909 m below the ground level. The material between 60 m and 909 m is denoted as soft-rock and its effects on the earthquake motions are included in the input synthetic earthquake time history. Figure 2-1 also

Depth (m)				
0				
		MEDIUM DENSE SM-SP		
	γ_s = 19.6 kN/m^3	D_r = 0.502, 0.668, 0.761		N_{SPT} = 7-16
2.9				
		STIFF ML-CL		
	γ_s = 19.6 kN/m^3	PI = 10-20	S_u = 89.7 kN/m^2	N_{SPT} =15
5.5				
		MEDIUM DENSE SM-SC		
	γ_s = 18.9 kN/m^3	D_r = 0.423, 0.511, 0.588		N_{SPT} = 9-17
11.6				
		MEDIUM DENSE SP		
	γ_s = 19.6 kN/m^3	D_r = 0.405, 0.521, 0.618		N_{SPT} = 11-25
17.7				
		DENSE SP-GP		
	γ_s = 21.2 kN/m^3	D_r = 0.713, 0.757, 0.786		N_{SPT} = 40-49
19.2				
		STIFF CL		
	γ_s = 20.4 kN/m^3	PI = 20-40	S_u = 95.8 kN/m^2	N_{SPT} =16
23.2				
		DENSE SP		
	γ_s = 21.2 kN/m^3	D_r = 0.90		
27.5				
		VERY STIFF CL		
	γ_s = 20.4 kN/m^3	PI = 20-40	S_u = 119.7 kN/m^2	
29.3				
		DENSE SC		
	γ_s = 21.2 kN/m^3	D_r = 0.84		
36.9				
		VERY DENSE SP		
	γ_s = 22.0 kN/m^3	D_r = 0.925		
46.4				
		VERY STIFF CL		
	γ_s = 20.4 kN/m^3	PI = 20-40	S_u = 192.0 kN/m^2	
53.4				
		VERY STIFF CL		
	γ_s = 20.4 kN/m^3	PI = 20-40	S_u = 215.4 kN/m^2	
60.0				

FIGURE 2-1 Soil Profile of a Site at President Island

shows the basic soil properties such as total unit weights γ_s of both sand and clay, plasticity index PI of clay, and the range of standard penetration test blowcounts N_{SPT} obtained from existing boring logs. The relative density for sand D_r, which has significant effects on the soil liquefaction potential, is estimated from the corrected standard penetration test blowcount $(N_1)_{60}$ based on the relationship suggested by Tokimatsu and Seed [9] (figure 2-2). $(N_1)_{60}$ is obtained by normalizing the N_{SPT} value to an effective overburden pressure of 1 tsf (95.8 kN/m^2) and an effective energy delivered to the drill rod at 60% of the ideal free-fall energy [10].

$$(N_1)_{60} = C_N \times C_F \times N_{SPT} \tag{2.1}$$

where C_F is a factor for correcting percentage of energy delivered to the drill rod. C_F is equal to 1.0 for rope and pulley type and 0.85 for donut type. C_N is a factor for correcting the overburden pressure.

$$C_N = 1 - 1.25 \log \left(\frac{\sigma'_0}{\sigma_1}\right) \tag{2.2}$$

where σ_1 is equal to 1 tsf (95.8 kN/m^2) and σ'_0 is the effective vertical confining (overburden) pressure.

2.1.1 Hysteretic Behavior

Soil exhibits pronounced nonlinear behavior under cyclic loadings. The secant shear modulus G is strain-dependent and decreases with increasing

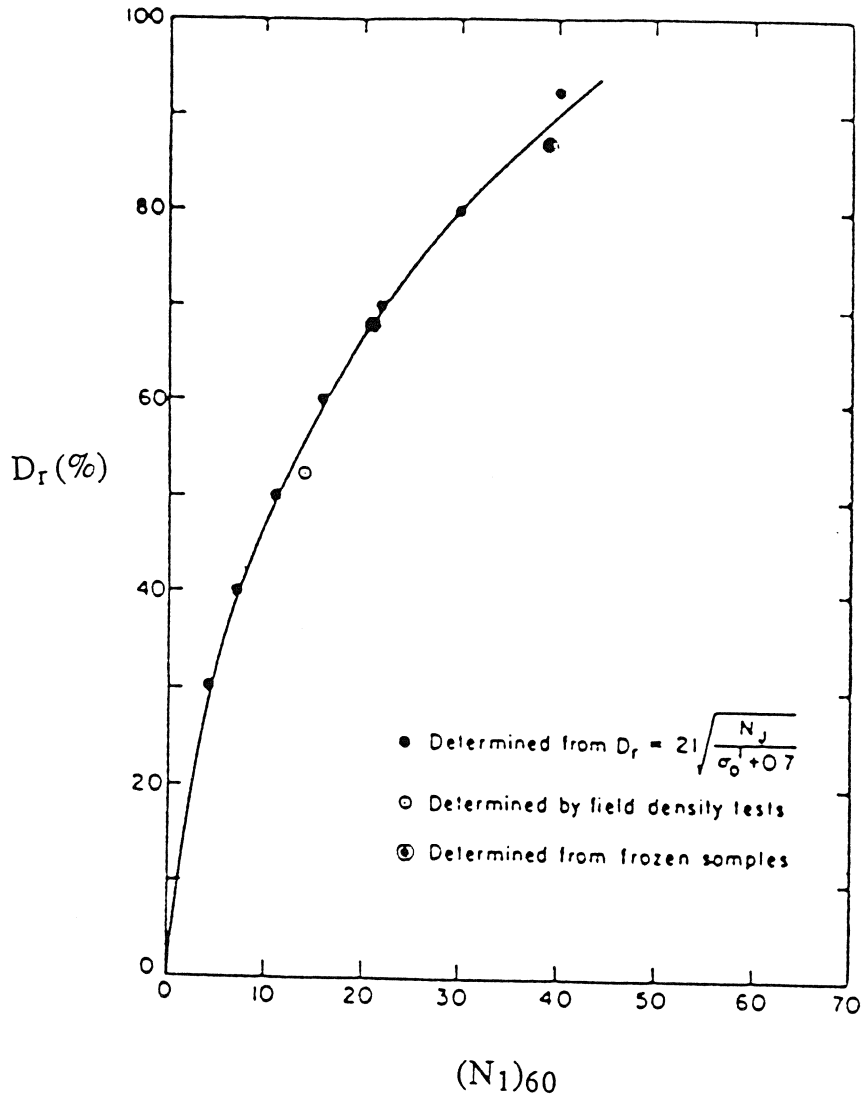

FIGURE 2-2 Relationship Between Relative Density and $(N_1)_{60}$ (after Tokimatsu and Seed 1986)

shear strain γ. In the MASH program, the secant shear modulus is expressed as

$$\frac{G}{G_o} = 1 - \left[\frac{[\gamma/\gamma_o]^{2B}}{1 + [\gamma/\gamma_o]^{2B}}\right]^A \tag{2.3}$$

where G_o is the low-strain shear modulus; γ_o is the reference strain; and A and B are two parameters that define the shape of the shear modulus reduction curve.

The secant shear modulus for sand is affected primarily by the confining pressure and relative density [11-14]. The low-strain shear modulus G_o is usually taken as the shear modulus corresponding to a strain level of 10^{-6} or less. In the MASH program, G_o in psf is estimated from the following empirical equation [8]:

$$G_o = 61000\ [1 + 0.01\ (D_r - 75)]\ (\bar{\sigma})^{1/2} \tag{2.4}$$

where D_r is the relative density in percentage and $\bar{\sigma}$ is the average effective confining pressure in psf.

The reference strain γ_o is expressed as

$$\gamma_o = \frac{\tau_{max}}{G_o} \tag{2.5}$$

where τ_{max} is the maximum shear stress under dynamic loadings and is computed using the formula suggested by Hardin and Drnevich [15].

The parameters A and B in equation (2.3) define the shape of the shear modulus reduction curve. Hwang and Lee [16] determined the values of A and B for sand based on experimental data available in the literature (figure 2-3). The parameters A and B corresponding to the mean, mean plus one standard deviation (SD), and mean minus one SD curves are shown in table 2-I. The lower and upper bound values are also included in the table. On the basis of these parameters values, the shear modulus reduction curves for sand are shown in figure 2-3.

Table 2-I Parameter Values of A and B for Sand

Curves	A	B
Lower	0.509	0.480
Mean - SD	0.705	0.445
Mean	0.941	0.441
Mean + SD	1.268	0.446
Upper	1.775	0.489

Several studies [17-19] have indicated that the plasticity index PI is the dominant factor affecting the shape of shear modulus reduction curve for clay. In general, as the plasticity index of clay increases, the shear modulus reduction curve gradually shifts to the right, indicating a small reduction of shear modulus with increasing plasticity index at the same strain level.

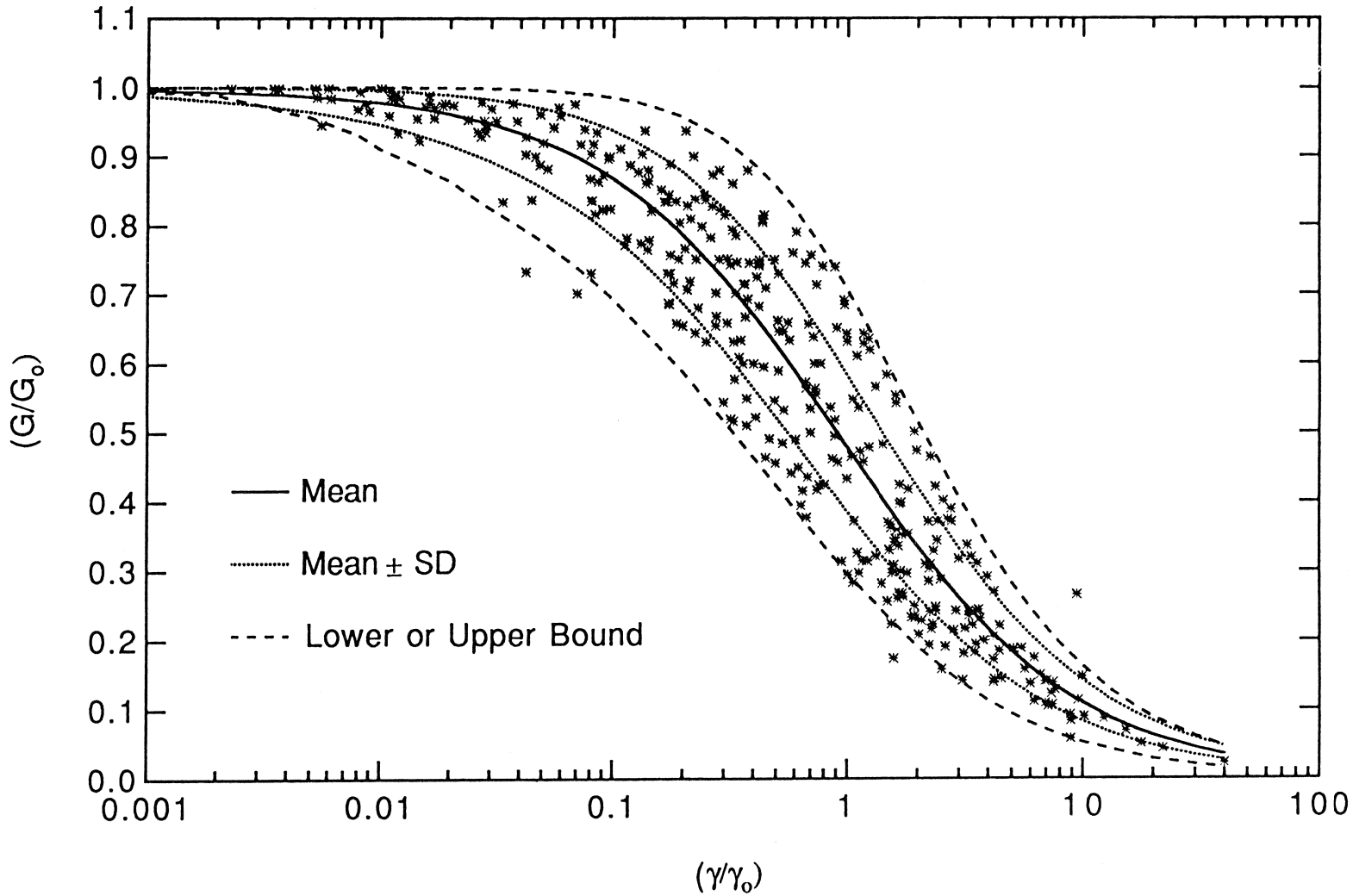

FIGURE 2-3 Shear Modulus Reduction Curves for Sand

The low-strain shear modulus G_o for clay in the MASH program is computed as [8]

$$G_o = 2500\ S_u \tag{2.6}$$

where S_u is the undrained shear strength of clay. In this study, τ_{max} is taken as S_u and G_o is taken as 2500 S_u; thus, the reference strain γ_o is equal to 0.0004.

Figure 2-4 shows the shear modulus reduction curves for clay corresponding to different ranges of plasticity indices suggested by Sun et al. [19]. The parameters A and B corresponding to these curves determined from nonlinear regression analyses by Hwang and Lee [16] are listed in table 2-II.

Table 2-II Parameter Values of A and B for Clay

PI	Curve	A	B
5-10	Mean	1.026	0.458
10-20	Mean	1.464	0.433
20-40	Mean	1.838	0.376
40-80	Mean	2.197	0.330
> 80	Mean	2.591	0.268

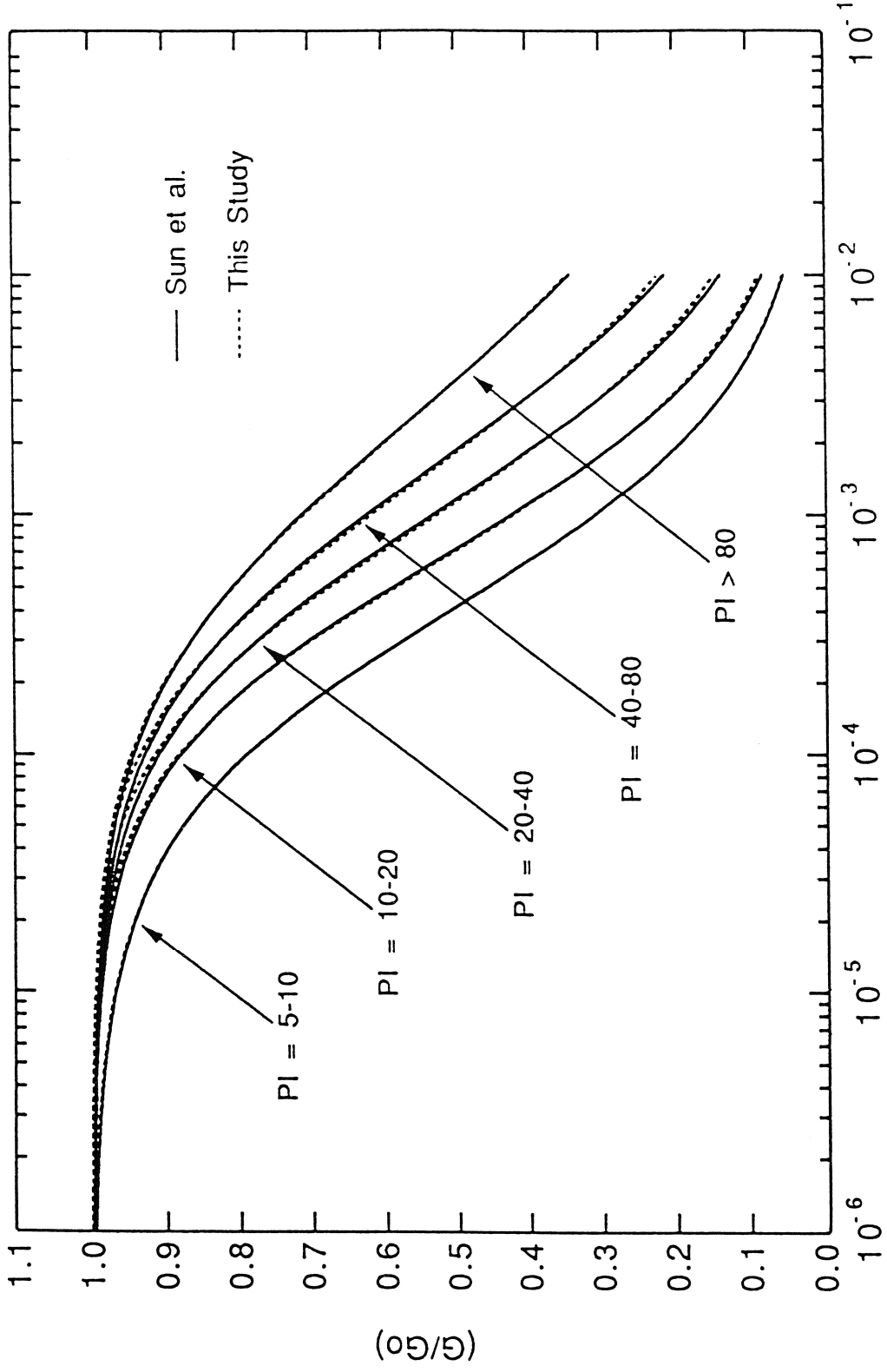

FIGURE 2-4 Shear Modulus Reduction Curves for Clay

2.1.2 Uncertainties in Site Parameters

From reviewing existing boring logs of the selected site, the clayey silts and silty clays are found to have a high clay content (>15%). These types of soils are not likely to liquefy in the event of an earthquake [7]. Thus, only sandy soils are considered potentially liquefiable in this study. For each liquefiable soil layer, uncertainties in two site parameters (relative density D_r and shear modulus G) are included in the probabilistic analysis.

The relative density D_r of a soil layer is estimated based on the corrected standard penetration test blowcount $(N_1)_{60}$, which in turn is computed from the N_{SPT} value. Thus, uncertainty in the D_r value is determined based on the range of N_{SPT} values established from the existing boring logs. Three D_r values (lower, mean, and upper) are estimated as shown in figure 2-1. These D_r values together with three pairs of parameters A and B (mean - SD, mean, and mean + SD) are used to quantify the uncertainty in shear modulus G. Thus, nine dynamic soil models are constructed as shown in table 2-III.

Table 2-III Parameters of Site Models

Site Model	Relative Density	Shear Modulus
1	Lower	Lower
2	Mean	Lower
3	Upper	Lower
4	Lower	Mean
5	Mean	Mean
6	Upper	Mean
7	Lower	Upper
8	Mean	Upper
9	Upper	Upper

2.2 Input Base Motions

Seismic hazards in Memphis, Tennessee, are entirely dominated by the New Madrid seismic zone (NMSZ) (figure 2-5). In this study, the seismic source of hypothetical New Madrid earthquakes is assumed at Marked Tree, Arkansas, which is near the southern end of the NMSZ. The epicentral distance from the seismic source to the site at President Island is about 57 km. Both seismic source and the site are indicated in figure 2-5. In this study, a seismologically based model is used to generate synthetic acceleration time histories. This model is briefly described below.

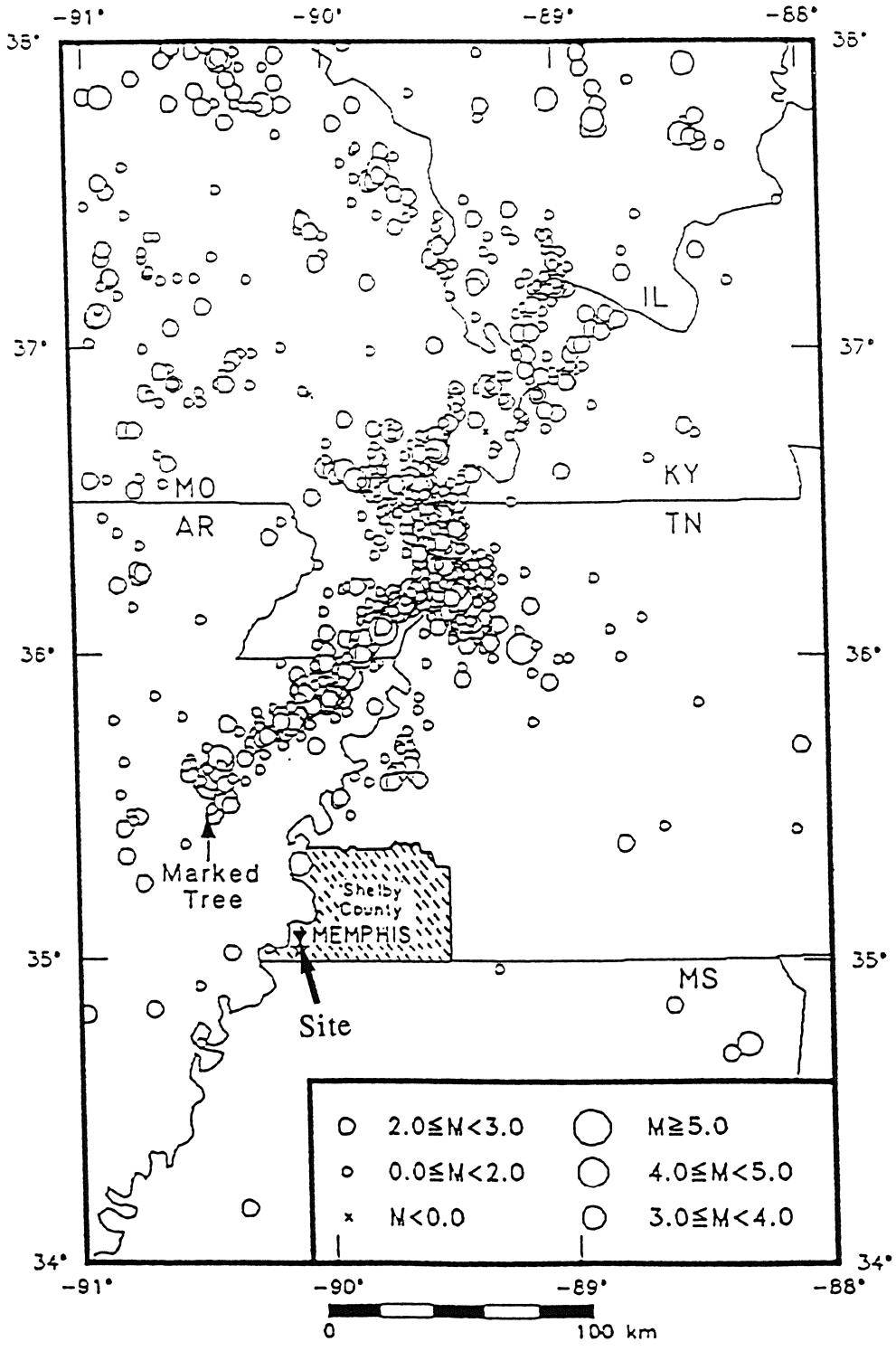

FIGURE 2-5 Locations of Seismic Source and Site

2.2.1 Fourier Acceleration Amplitude Spectrum

The Fourier acceleration amplitude spectrum at the base of a soil profile is expressed as follows [20-22]:

$$A(f) = C \times S(f) \times D(f) \times AF(f) \tag{2.7}$$

where C is a scaling factor; $S(f)$ is a source spectral function; $D(f)$ is a diminution function; and $AF(f)$ is an amplification factor.

The source spectral function $S(f)$ used in this study is a ω^2 source acceleration spectrum proposed by Brune [23]. The source spectrum is expressed in terms of the corner frequency f_0 and seismic moment M_0:

$$S(f) = (2\pi f)^2 \frac{M_0}{1+(\frac{f}{f_0})^2} \tag{2.8}$$

The corner frequency f_0 is related to the seismic moment M_0 through the shear-wave velocity at the source region β and stress parameter $\Delta\sigma$:

$$f_0 = 4.9 \times 10^6 \beta(\frac{\Delta\sigma}{M_0})^{1/3} \tag{2.9}$$

The scaling factor C accounts for the shear-wave radiation pattern.

$$C = \frac{<R_{\theta\phi}> V}{4 \pi \rho \beta^3} \cdot \frac{1}{r} \tag{2.10}$$

where $<R_{\theta\phi}>$ = radiation pattern; V = partition of a vector into horizontal components; ρ = crustal density; and r = hypocentral distance. $<R_{\theta\phi}>$ is the radiation pattern corresponding to different types of seismic waves over a range of azimuths θ and take-off angles ϕ. For ϕ and θ averaged over the whole focal sphere, the shear-wave radiation pattern $<R_{\theta\phi}>$ is 0.55 [24]. V is the factor that accounts for the partition of a vector into horizontal components and is chosen as $1/\sqrt{2}$. On the basis of the hypocentral locations of instrumentally recorded microearthquakes in the NMSZ, the average focal depth of 10 km is used. The crustal density ρ of continental crust at this focal depth is taken as 2.7 gm/cm^3 and the shear-wave velocity β is 3.5 km/sec.

The diminution function $D(f)$ represents the anelastic attenuation that accounts for the damping of the earth's crust and a sharp decrease of acceleration spectra above a cutoff frequency f_m.

$$D(f) = \exp\left[\frac{-\pi f r}{Q(f)\,\beta}\right] P(f,f_m) \qquad (2.11)$$

where $Q(f)$ = frequency-dependent quality factor; and $P(f,f_m)$ = high-cut filter. The quality factor $Q(f)$ describes the attenuation of seismic waves and is frequency dependent. Dwyer et al. [25] conducted an attenuation study in the central United States and suggested the quality factor of shear and Lg waves as

$$Q(f) = 1500\, f^{0.40} \qquad (2.12)$$

The high-cut filter $P(f, f_m)$ accounts for the observation that the acceleration spectra often show a sharp decrease above a cutoff frequency f_m, which cannot be attributed to path attenuation. In this study, a Butterworth filter with a cutoff frequency of 30 Hz is used.

The amplification factor $AF(f)$ accounts for the soft-rock effects resulting from the decreasing shear-wave velocities in the soft-rock layers. $AF(f)$ can be calculated as [22]

$$AF(f) = \sqrt{\frac{\beta}{\beta_r}} \tag{2.13}$$

where β is the shear-wave velocity at the source and β_r is the effective shear-wave velocity. The cumulative travel time T_n of the upper n layers measured from the base of soil profile is computed as

$$T_n = \sum_{i=1}^{n} \frac{H_i}{\beta_i} \tag{2.14}$$

where β_i and H_i are the shear-wave velocity and thickness of the i-th layer, respectively. The wave frequency f_n of the upper n layers is calculated as $f_n = 1/(4T_n)$. The effective shear-wave velocity β_r corresponding to the wave frequency f_n is

$$(\beta_r)_n = 4.0 \times f_n \times H_n \tag{2.15}$$

where H_n is the total depth of the upper n layers. For each frequency f_n, the corresponding amplification factor AF(f) can be computed using equation (2.13). Thus, the amplification factor AF(f) is frequency-dependent. By using the shear-wave velocity and thickness of soft-rock layers in the Memphis area as suggested by Jacob et al. [26], the amplification factors for the selected site are calculated and shown in table 2-IV.

Table 2-IV Calculation of Amplification Factors

H_i (m)	ΣH_i (m)	β_i (m/s)	T_n (sec)	f_n (Hz)	β_r (m/s)	AF
9	9	400	0.02225	11.11	400.00	2.96
13	22	600	0.04392	5.69	500.95	2.64
17	39	1000	0.06092	4.10	640.22	2.34
100	139	950	0.16618	1.50	836.44	2.04
300	439	1100	0.43891	0.57	1000.89	1.87
200	639	1400	0.58176	0.43	1129.91	1.76
200	839	1700	0.69941	0.36	1197.00	1.71
100	939	2000	0.74941	0.33	1254.98	1.67
2000	2939	3000	1.41607	0.18	2071.00	1.30
7061	10000	3500	3.43350	0.07	2892.60	1.10

2.2.2 Power Spectrum

An earthquake accelerogram generally shows a build-up segment followed by a strong-motion segment and then a decay segment. The frequency content of an earthquake accelerogram is found to be approximately

constant during the strong-motion segment. Thus, the strong-motion segment of an acceleration time history is considered as a stationary random process and the one-sided power spectrum $S_a(f)$ can be derived from the Fourier amplitude spectrum.

$$S_a(f) = \frac{2}{T_e} |A(f)|^2 \tag{2.16}$$

where $A(f)$ is the Fourier amplitude spectrum (equation 2.7) and T_e is the strong-motion duration.

2.2.3 Synthetic Acceleration Time Histories

In this study, the synthetic time histories are generated using the method proposed by Shinozuka [27]. Given the power spectrum, the stationary acceleration time histories $a_s(t)$ can be generated as follows:

$$a_s(t) = \sqrt{2} \sum_{k=1}^{N} \sqrt{S_a(\omega_k)\Delta\omega}\ \cos(\omega_k t + \phi_k) \tag{2.17}$$

where $S_a(\omega_k)$ = one-sided earthquake power spectrum; N = number of frequency intervals; $\Delta\omega$ = frequency increment; $\omega_k = k\,\Delta\omega$; and ϕ_k = random phase angles uniformly distributed between 0 and 2π. The nonstationary acceleration time histories a(t) can then be obtained from the multiplication of an envelope function w(t).

$$a(t) = a_s(t)w(t) \tag{2.18}$$

The envelope function w(t) proposed by Hwang et al. [28] is used in this study and is composed of three segments: (1) a parabolically increased segment simulating the initial-rise part of the accelerogram with its duration chosen as one fifth of T_e, (2) a constant segment representing the strong-motion portion of an earthquake excitation with a duration equal to T_e, and (3) a linearly decayed segment extending four fifths of T_e. Thus, the total duration is $2T_e$. Real earthquake records are commonly observed with long coda durations; however, the coda durations are considered unimportant in most engineering applications.

2.2.4 Uncertainties in Seismic Parameters

The seismologically based model for the horizontal accelerations at the base of a soil column is defined by several seismic parameters as summarized in table 2-V. Under a specific moment magnitude, epicentral distance, and quality factor, some parameters such as the crustal density ρ, shear-wave velocity β, and cut-off frequency f_m appear to have less influence on the resulting horizontal accelerations. On the other hand, the stress parameter $\Delta\sigma$ and strong-motion duration T_e have significant effects on the accelerations. Thus, uncertainties in these two parameters, $\Delta\sigma$ and T_e, are included in the analysis.

TABLE 2-V Seismic Parameters

Item	Symbol	Value
Moment magnitude	M	varied
Epicentral distance	R	57 km
Focal depth	h	10 km
Radiation pattern	$<R_{\theta\phi}>$	0.55
Horizontal component	V	0.71
Shear-wave velocity	β	3.5 km/sec
Source-rock density	ρ	2.7 gm/cm^3
Quality factor	$Q(f)$	$1500f^{0.4}$
Stress parameter	$\Delta\sigma$	varied
Cutoff frequency	f_m	30 Hz
Strong-motion duration	T_e	varied

For central and eastern North America, Boore and Atkinson [21] and McGuire et al. [29] suggested an average $\Delta\sigma$ of 100 bars. From the 1988 Saguenay earthquake, Atkinson and Boore [30] determined a stress parameter of about 200 bars. Thus, three values, 100, 150, and 200 bars, are used to represent the uncertainty in stress parameter.

In this study, the strong-motion duration T_e is equal to the source duration, which is the reciprocal of the corner frequency f_0 [31].

$$T_e = 1 / f_0 \qquad (2.19)$$

Using this equation, the strong-motion duration T_e for an **M** = 7.5 earthquake with $\Delta\sigma$ = 150 bars is about 14 seconds. According to the studies conducted by Johnston [32], Krinitzsky et al. [33], and Lai [34], the strong-motion duration has significant variation. Thus, the coefficient of variation is selected as 50% and the three values of 7, 14, and 21 seconds are chosen as representative values. For **M** = 6.5, 7.0, 7.5, and 8.0 New Madrid earthquakes, three representative values of T_e are shown in table 2-VI.

Table 2-VI Representative Values of Strong-Motion Duration

M	T_e (sec)
6.5	2.5, 5.0, 7.5
7.0	4.0, 8.0, 12.0
7.5	7.0, 14.0, 21.0
8.0	12.0, 24.0, 36.0

From the combination of three representative values of two seismic parameters, $\Delta\sigma$ and T_e, nine earthquake models are established. As an example, the nine models for an **M** = 7.5 earthquake are shown in table 2-VII. From each model, nine earthquake time histories are generated by using different random phase angles. Thus, a total of 81 earthquake time histories is generated for each moment magnitude. For an **M** = 7.5

earthquake, the peak base acceleration (PBA) of these 81 time histories are also listed in table 2-VII. The values of PBA vary significantly for each combination of stress drop $\Delta\sigma$ and strong-motion duration T_e.

Table 2-VII Parameters of Earthquake Models (**M** = 7.5)

EQ. Model	$\Delta\sigma$ (bars)	T_e (sec)	PBA (g)
1	100	7	0.362 - 0.474
2	100	14	0.241 - 0.321
3	100	21	0.228 - 0.261
4	150	7	0.441 - 0.540
5	150	14	0.325 - 0.404
6	150	21	0.264 - 0.360
7	200	7	0.500 - 0.733
8	200	14	0.408 - 0.549
9	200	21	0.329 - 0.414

2.3 Earthquake-Site Samples

From the combination of nine site models and nine earthquake models (81 synthetic horizontal acceleration time histories), 81 earthquake-site samples are established. As an example, the 81 earthquake-site samples for an **M** = 7.5 earthquake is shown in table 2-VIII.

Table 2-VIII Earthquake-Site Samples

Sample	EQ. Model	$\Delta\sigma$ (bars)	T_e (sec)	Site Model	$(N_1)_{60}$ or D_r	A and B
1	1	100	7	1	Lower	Lower
2	1	100	7	2	Mean	Lower
3	1	100	7	3	Upper	Lower
4	1	100	7	4	Lower	Mean
5	1	100	7	5	Mean	Mean
6	1	100	7	6	Upper	Mean
7	1	100	7	7	Lower	Upper
8	1	100	7	8	Mean	Upper
9	1	100	7	9	Upper	Upper
10	2	100	14	1	Lower	Lower
11	2	100	14	2	Mean	Lower
12	2	100	14	3	Upper	Lower
13	2	100	14	4	Lower	Mean
14	2	100	14	5	Mean	Mean
15	2	100	14	6	Upper	Mean
16	2	100	14	7	Lower	Upper
17	2	100	14	8	Mean	Upper
18	2	100	14	9	Upper	Upper
19	3	100	21	1	Lower	Lower
20	3	100	21	2	Mean	Lower
21	3	100	21	3	Upper	Lower
22	3	100	21	4	Lower	Mean
23	3	100	21	5	Mean	Mean
24	3	100	21	6	Upper	Mean
25	3	100	21	7	Lower	Upper
26	3	100	21	8	Mean	Upper
27	3	100	21	9	Upper	Upper

Table 2-VIII Earthquake-Site Samples (Continued)

Sample	EQ. Model	$\Delta\sigma$ (bars)	T_e (sec)	Site Model	$(N_1)_{60}$ or D_r	A and B
28	4	150	7	1	Lower	Lower
29	4	150	7	2	Mean	Lower
30	4	150	7	3	Upper	Lower
31	4	150	7	4	Lower	Mean
32	4	150	7	5	Mean	Mean
33	4	150	7	6	Upper	Mean
34	4	150	7	7	Lower	Upper
35	4	150	7	8	Mean	Upper
36	4	150	7	9	Upper	Upper
37	5	150	14	1	Lower	Lower
38	5	150	14	2	Mean	Lower
39	5	150	14	3	Upper	Lower
40	5	150	14	4	Lower	Mean
41	5	150	14	5	Mean	Mean
42	5	150	14	6	Upper	Mean
43	5	150	14	7	Lower	Upper
44	5	150	14	8	Mean	Upper
45	5	150	14	9	Upper	Upper
46	6	150	21	1	Lower	Lower
47	6	150	21	2	Mean	Lower
48	6	150	21	3	Upper	Lower
49	6	150	21	4	Lower	Mean
50	6	150	21	5	Mean	Mean
51	6	150	21	6	Upper	Mean
52	6	150	21	7	Lower	Upper
53	6	150	21	8	Mean	Upper
54	6	150	21	9	Upper	Upper

Table 2-VIII Earthquake-Site Samples (Continued)

Sample	EQ. Model	$\Delta\sigma$ (bars)	T_e (sec)	Site Model	$(N_1)_{60}$ or D_r	A and B
55	7	200	7	1	Lower	Lower
56	7	200	7	2	Mean	Lower
57	7	200	7	3	Upper	Lower
58	7	200	7	4	Lower	Mean
59	7	200	7	5	Mean	Mean
60	7	200	7	6	Upper	Mean
61	7	200	7	7	Lower	Upper
62	7	200	7	8	Mean	Upper
63	7	200	7	9	Upper	Upper
64	8	200	14	1	Lower	Lower
65	8	200	14	2	Mean	Lower
66	8	200	14	3	Upper	Lower
67	8	200	14	4	Lower	Mean
68	8	200	14	5	Mean	Mean
69	8	200	14	6	Upper	Mean
70	8	200	14	7	Lower	Upper
71	8	200	14	8	Mean	Upper
72	8	200	14	9	Upper	Upper
73	9	200	21	1	Lower	Lower
74	9	200	21	2	Mean	Lower
75	9	200	21	3	Upper	Lower
76	9	200	21	4	Lower	Mean
77	9	200	21	5	Mean	Mean
78	9	200	21	6	Upper	Mean
79	9	200	21	7	Lower	Upper
80	9	200	21	8	Mean	Upper
81	9	200	21	9	Upper	Upper

SECTION 3

SITE LIQUEFACTION POTENTIAL

The liquefaction potential of a soil layer is affected by site parameters such as relative density, shear modulus, percentage of clay, effective confining pressure, grain-size distribution, depth of water table, and age of deposition [7]. In addition, it is also affected by seismic parameters such as the amplitude, frequency content, and duration of an earthquake.

3.1 Factor of Safety against Liquefaction

The factor of safety against liquefaction F_L of a soil layer is defined as

$$F_L = R/L \tag{3.1}$$

in which R is the resistance shear stress ratio and L is the shear stress ratio induced by an earthquake. For each potentially liquefiable layer, the earthquake-induced shear stress ratio L is evaluated from nonlinear site response analysis. The average shear stress τ_{av} is defined as [7]:

$$\tau_{av} = 0.65\ \tau_{max} \tag{3.2}$$

and then the shear stress ratio L is determined as

$$L = \tau_{av}/\sigma'_0 \tag{3.3}$$

where σ'_0 is the effective vertical confining (overburden) pressure. The irregular shear stress time history of each potentially liquefiable layer obtained from nonlinear site response analysis is converted into equivalent uniform cycles N_{eq} at the average shear stress ratio τ_{av}/σ'_0 based on the procedure proposed by Seed et al. [3]. The equivalent uniform cycles N_{eq} is computed as follows:

$$N_{eq} = \sum_{i=1}^{n} (N_i/N_{Li})\, N_{ref} \tag{3.4}$$

where N_i is the number of induced shear stress cycles at the shear stress ratio of τ_i/σ'_0 and N_{Li} is the number of equivalent uniform cycles required to cause liquefaction at the same shear stress ratio. N_{ref} is the number of equivalent uniform shear stress cycles required to cause liquefaction at the average shear stress ratio. The values of N_{Li} and N_{ref} can be determined from laboratory cyclic test data as shown in figure 3-1. The cyclic test data for sand (SP), silty sand (SM), and clayey sand (SC) used in this study are shown in figures 3-2 through 3-4, respectively [35-37]. By using the equivalent uniform cycles N_{eq} and relative density D_r, the resistance shear stress ratio R for either sand, silty sand, or clayey sand can be determined from these figures. Then, the factor of safety against liquefaction F_L of a soil layer can be calculated from the L and R values.

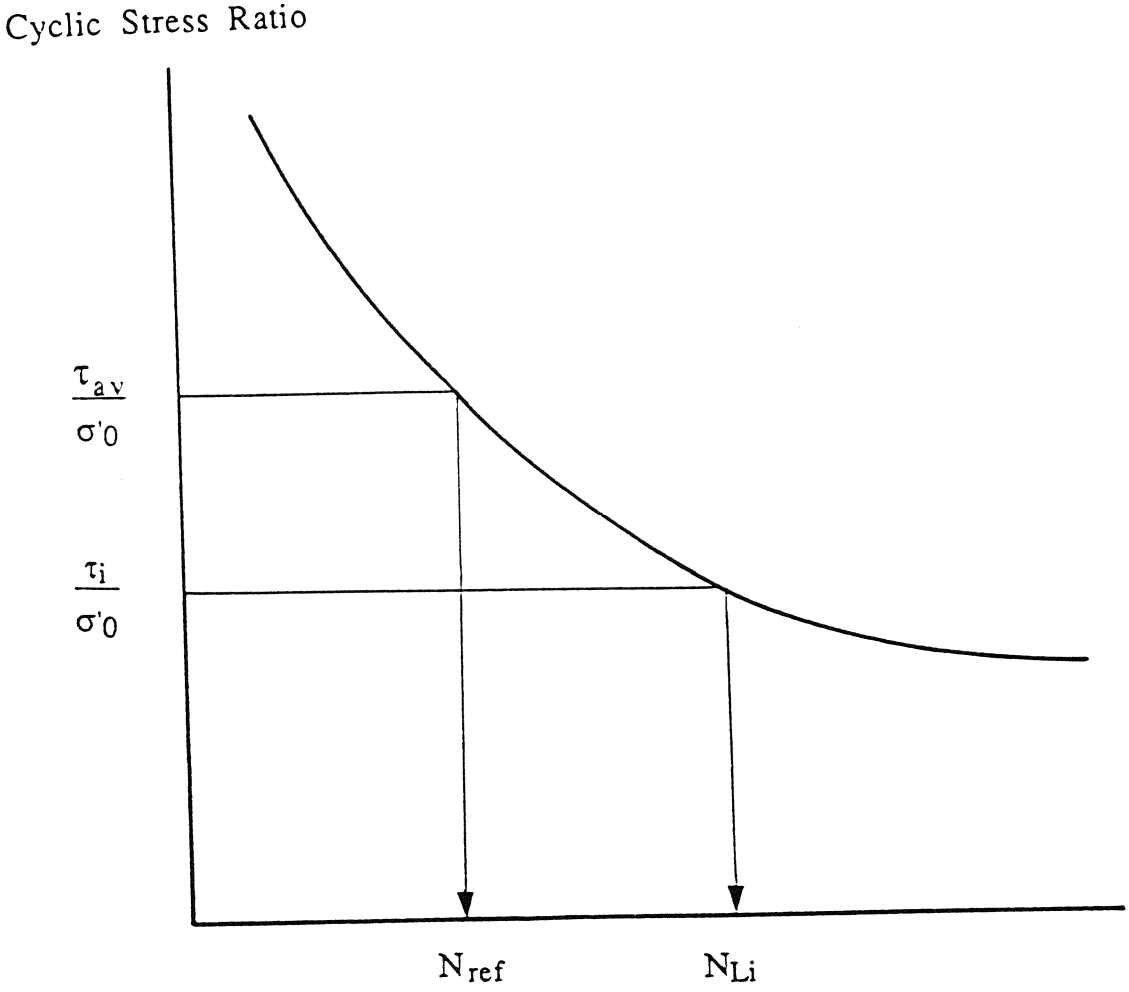

FIGURE 3-1 Determination of N_{ref} and N_{Li} Values

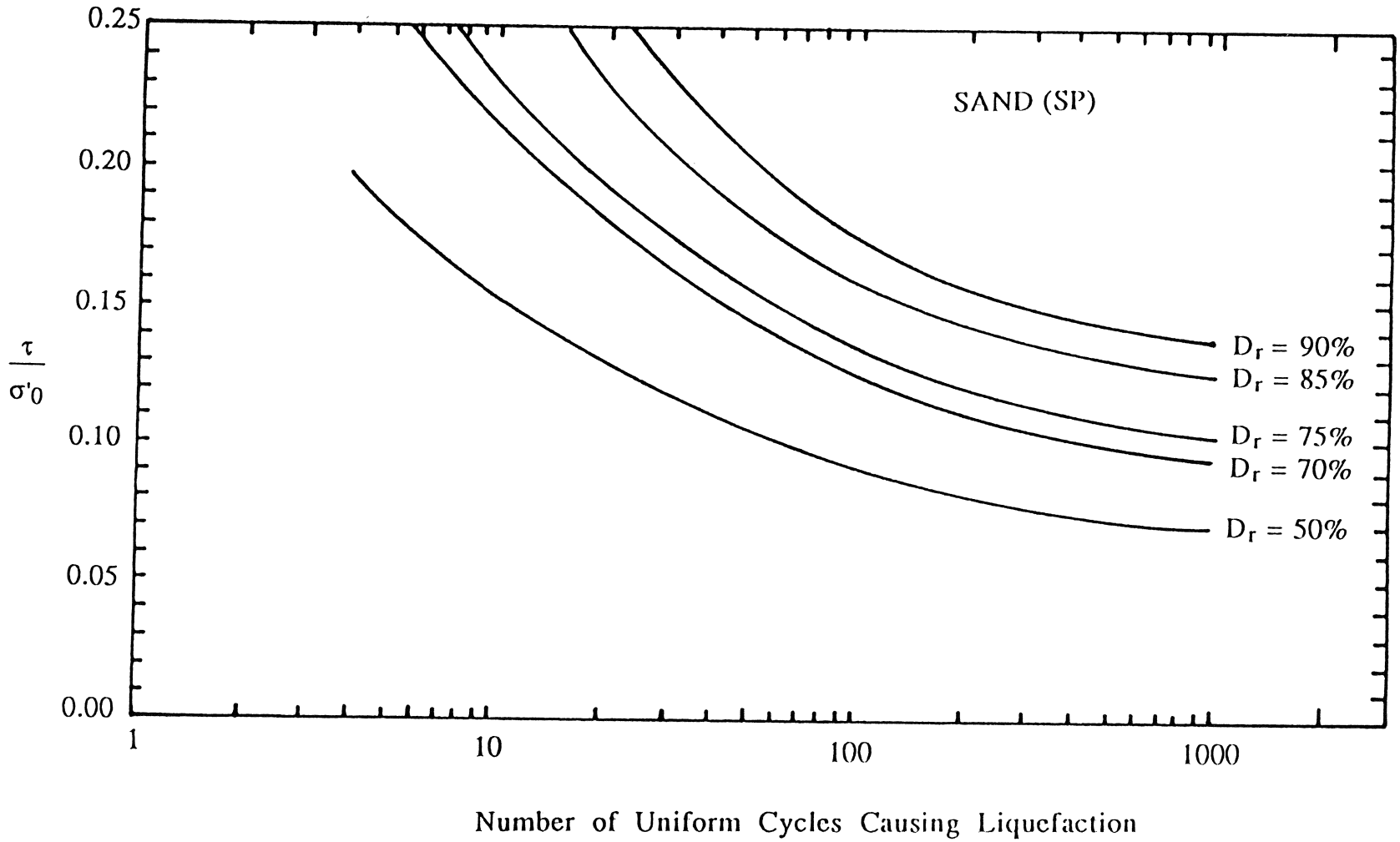

FIGURE 3-2 Cyclic Test Data for Sand (after Chang et al. 1990)

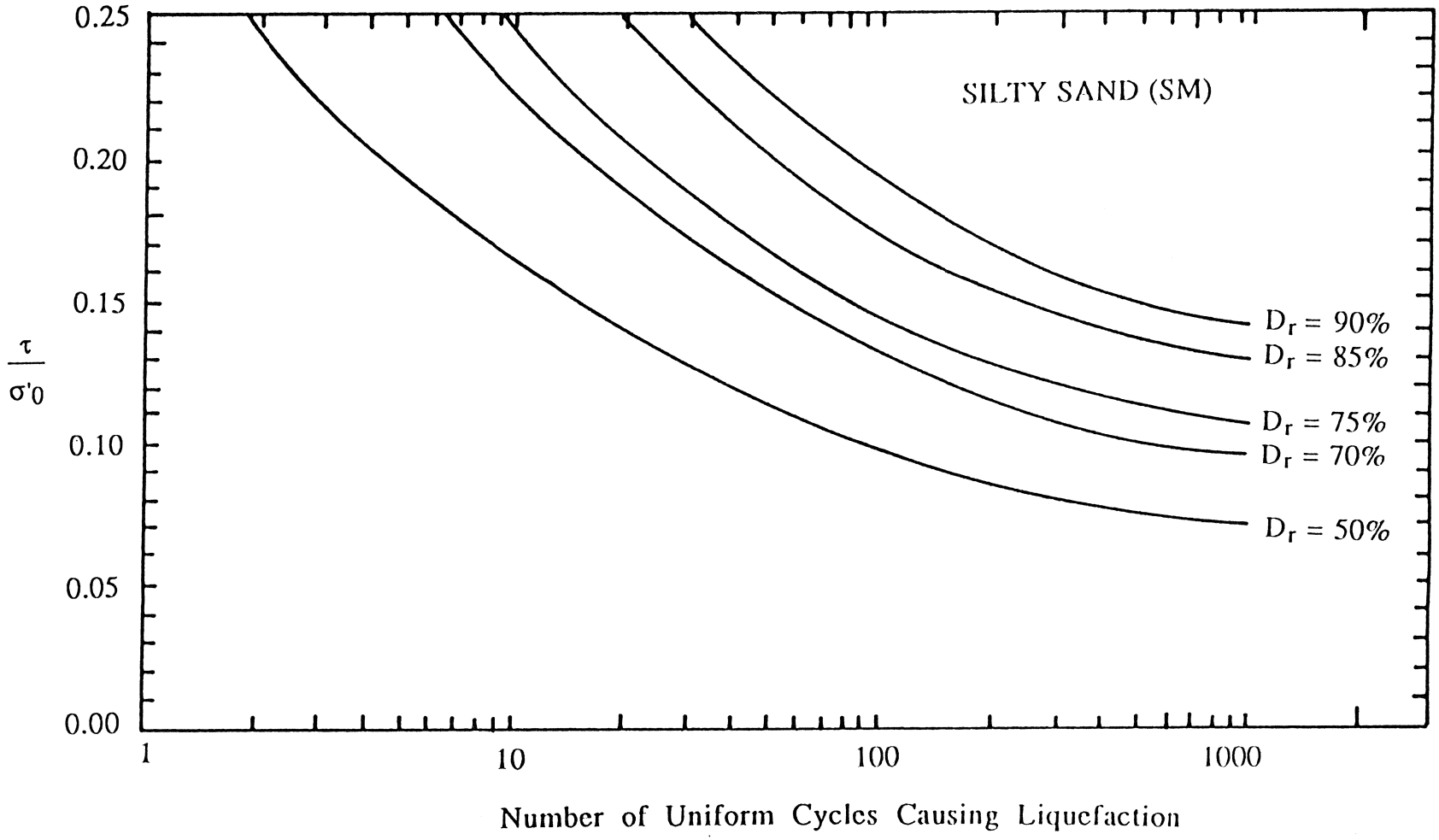

FIGURE 3-3 Cyclic Test Data for Silty Sand (after Chang et al. 1990)

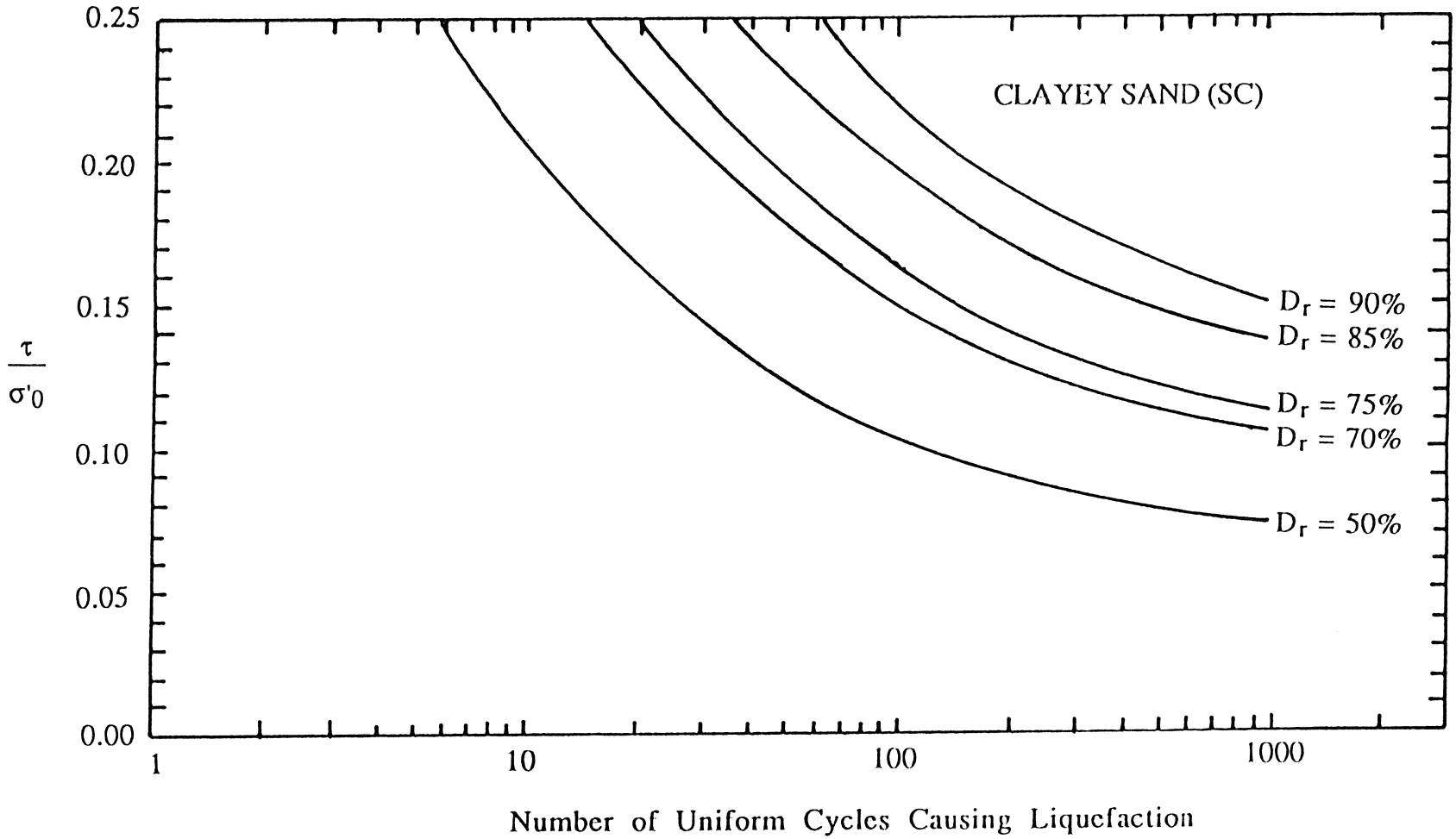

FIGURE 3-4 Cyclic Test Data for Clayey Sand (after Chang et al. 1990)

3.2 Liquefaction Potential Index

The F_L value only indicates the occurrence of liquefaction in a soil layer on a yes or no basis and does not reflect the liquefaction severity of a site. The liquefaction potential of a site is affected by the F_L value, thickness, and depth of liquefied layers in a soil profile. In this study, the liquefaction potential index P_L proposed by Iwasaki et al. [4] is used to quantify the liquefaction severity of a site.

$$P_L = \sum_{i=1}^{n} Q_i \times W_i \times H_i \tag{3.5}$$

where H_i is the thickness of the i-th layer in meter and Q_i accounts for the severity of the i-th liquefied layer.

$$Q_i = 1 - F_{Li} \qquad \text{for } F_{Li} \leq 1.0 \text{ (liquefied)} \tag{3.6}$$

$$Q_i = 0 \qquad \text{for } F_{Li} > 1.0 \text{ (non-liquefied)}$$

W_i accounts for the influence of depth of the i-th liquefied layer on the liquefaction severity of a site.

$$W_i = 10 - 0.5\, z \tag{3.7}$$

where z is the depth measured from the ground level in meter. The maximum depth considered in this study is 20 m. On the basis of the P_L

value, the liquefaction potential of a site is classified as no, minor, moderate, or major liquefaction as shown in table 3-I.

Table 3-I Liquefaction Potential Index P_L

P_L	Liquefaction Potential
0	No or little
$0 < P_L \leq 5$	Minor
$5 < P_L \leq 15$	Moderate
$15 < P_L$	Major

3.3 Illustration

The soil profile of sample 17 (table 2-VIII) is shown in table 3-II. Layers 1, 3, 4, and 5 (sandy soils) in the soil profile are identified as the potentially liquefiable layers. The shear-wave velocity of the soil layers is shown in figure 3-5. Figure 3-6 shows the horizontal acceleration time history at the base of the soil column from a moment magnitude 7.5 New Madrid earthquake. The time history is generated by using a stress drop of 100 bars and strong-motion duration of 14 seconds. The peak acceleration of this time history is 0.305 g. By using the MASH computer program, a nonlinear site response analysis is performed to obtain the shear stress time histories at the center of layers 1, 3, 4, and 5. The shear stress time history for layer 3 is shown in figure 3-7. As shown in the figure, the maximum shear stress τ_{max} is 546.0 psf (26.14 kN/m^2). The effective

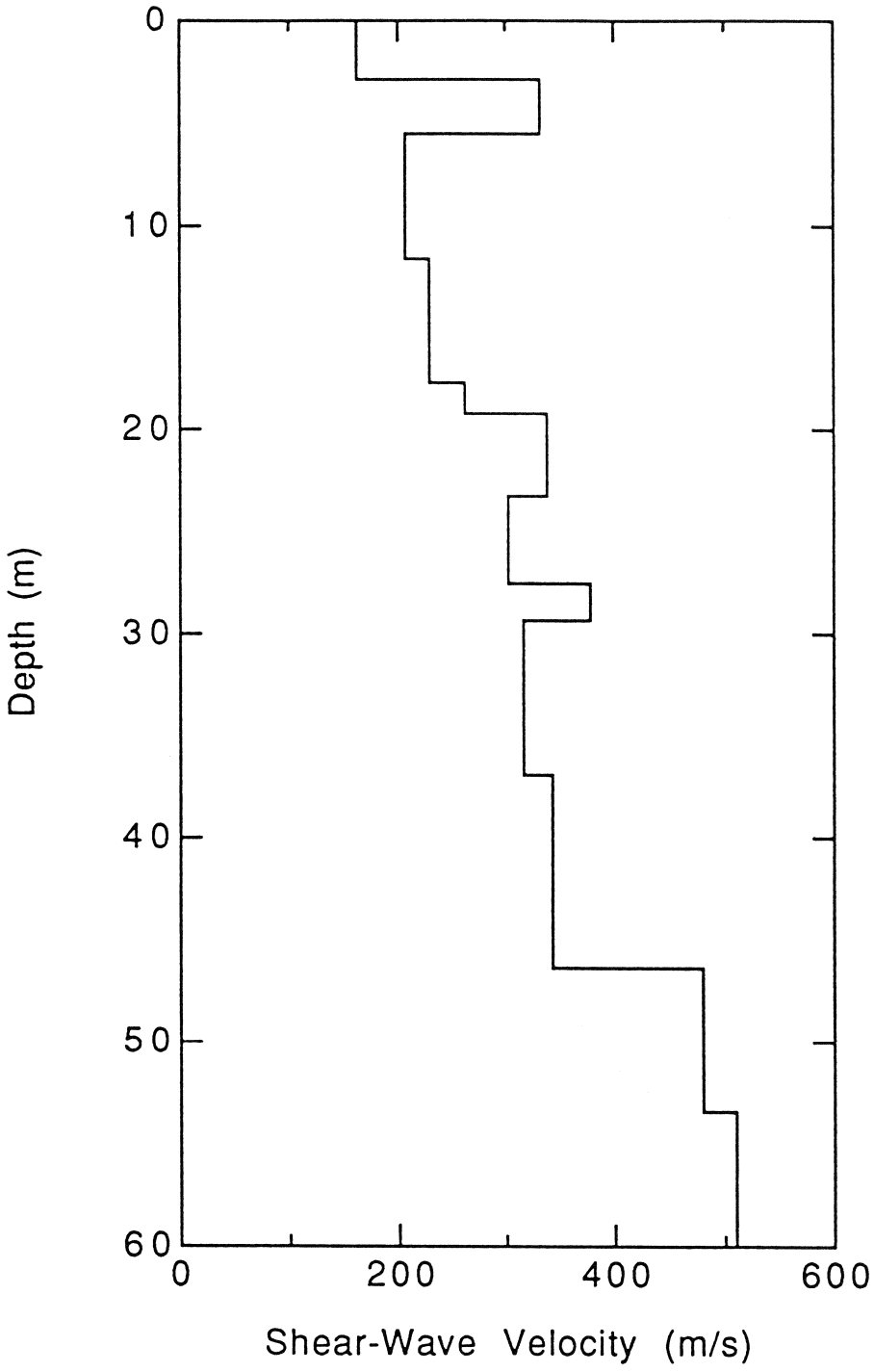

FIGURE 3-5 Shear-Wave Velocity of Soil Profile (Sample 17)

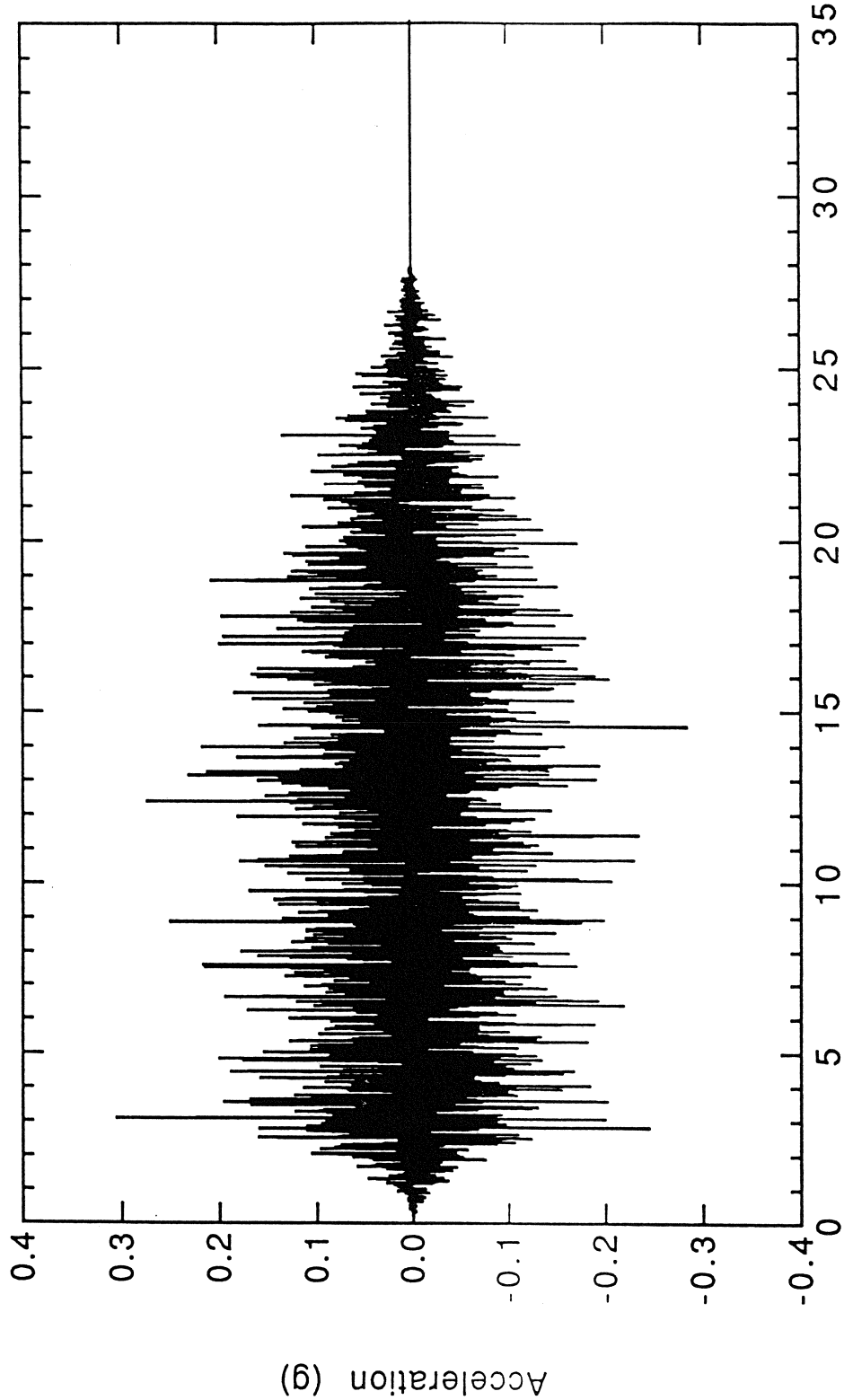

FIGURE 3-6 Base Acceleration Time History (Sample 17)

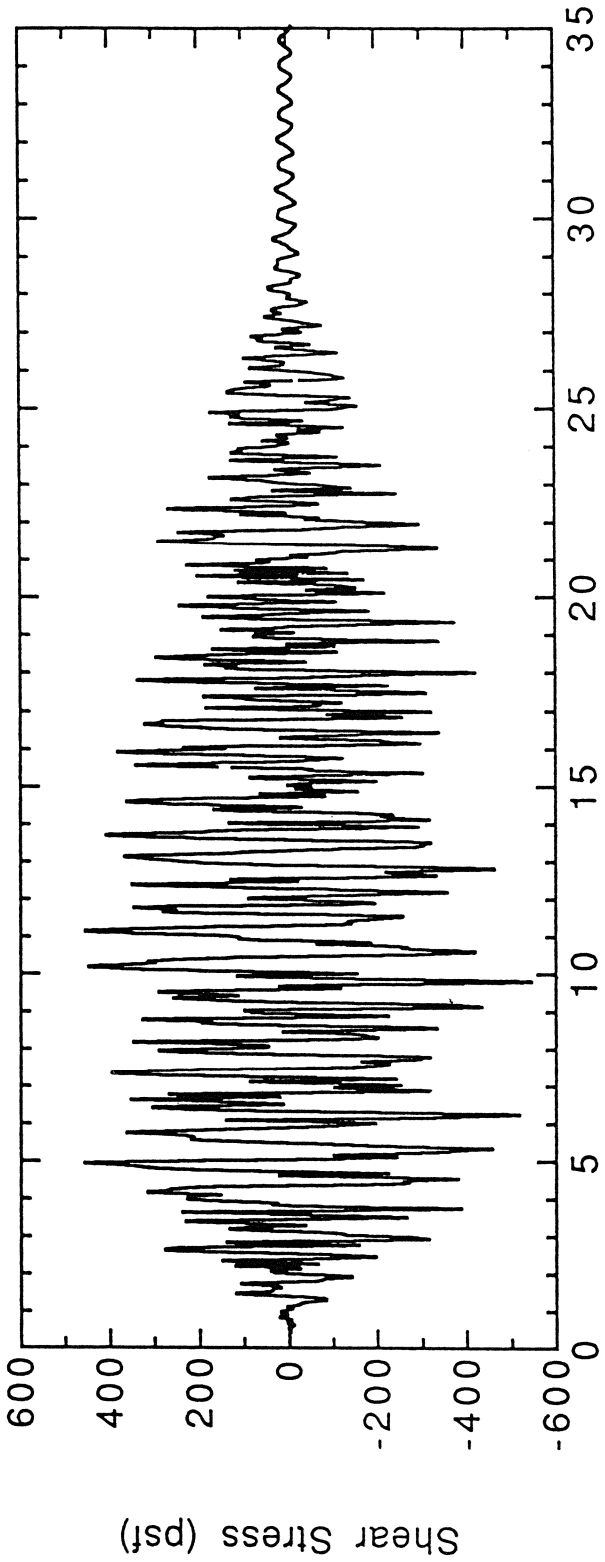

FIGURE 3-7 Shear Stress Time History of Layer 3 (Sample 17)

vertical confining pressure computed at the center of the layer is 2295.6 psf (109.9 kN/m^2). Using equations (3.2) and (3.3), the earthquake-induced shear stress ratio L is computed as

$$L = (0.65 \times 546.0 / 2295.6) = 0.155$$

For all potentially liquefiable layers, the earthquake-induced shear stress ratios L are shown in table 3-III.

Table 3-II Soil Profile for Sample 17

Layer	Soil Type	Thickness (m)	γ_s (kN/m^3)	N_{SPT}	D_r
1	SM-SP	2.9	19.6	12	0.67
2	ML-CL	2.6	19.6	15	-
3	SM-SC	6.1	18.9	13	0.51
4	SP	6.1	19.6	18	0.52
5	SP-GP	1.5	21.2	45	0.76
6	CL	4.0	20.4	16	-
7	SP	4.3	21.2	-	-
8	CL	1.8	20.4	-	-
9	SC	7.6	21.2	-	-
10	SP	9.5	22.0	-	-
11	CL	7.0	20.4	-	-
12	CL	6.6	20.4	-	-

Table 3-III Determination of P_L Value (Sample 17)

Layer	N_{eq} (cycles)	R	L	F_L	P_L
1	50	0.146	0.111	1.32	0.00
3	37	0.124	0.155	0.80	6.93
4	36	0.118	0.148	0.80	3.33
5	37	0.170	0.134	1.27	0.00
					Σ =10.26

The soil type of layer 3 is medium dense SM-SC; thus, figure 3-3 is used to determine the resistance shear stress ratio R. For the average shear stress ratio of 0.155, the number of equivalent uniform cycles required to cause liquefaction N_{ref} is 15.2 cycles obtained from the curve corresponding to D_r = 0.51 in figures 3-3. From equation (3.4), the equivalent uniform cycles N_{eq} for layer 3 is determined to be 37 cycles. On the basis of N_{eq} = 37 cycles and D_r = 0.51, the resistance shear stress ratio R for layer 3 obtained from figure 3-3 is equal to 0.124. The R values for layers 1, 4, and 5 are obtained by using the same procedure and are listed in table 3-III. From these R and L values, the factor of safety F_L for layers 1, 3, 4, and 5 are calculated as 1.32, 0.80, 0.80, and 1.27, respectively. On the basis of the F_L value, depth and thickness of the soil layers, the P_L value of the site is calculated to be 10.26. The P_L value of 10.26 indicates that the site will experience moderate liquefaction if an earthquake with moment magnitude of 7.5 occurs at Marked Tree, Arkansas.

SECTION 4

PROBABILISTIC LIQUEFACTION ANALYSIS

4.1 Liquefaction Potential Probability Matrix

For a specified moment magnitude M_i, 81 earthquake-site samples such as those shown in table 2-VIII are analyzed to determine the liquefaction potential index P_L of each earthquake-site sample. On the basis of the PL value, each sample can be classified as either no, minor, moderate, or major liquefaction. Then, the probabilities of no, minor, moderate, and major liquefaction can be calculated as follows:

$$P(no|M_i) = (N_{no}|M_i)/N \tag{4.1}$$

$$P(min|M_i) = (N_{min}|M_i)/N \tag{4.2}$$

$$P(mod|M_i) = (N_{mod}|M_i)/N \tag{4.3}$$

$$P(maj|M_i) = (N_{maj}|M_i)/N \tag{4.4}$$

where $P(no|M_i)$, $P(min|M_i)$, $P(mod|M_i)$, and $P(maj|M_i)$ denote the probability of no, minor, moderate, and major liquefaction, respectively given an M_i earthquake. $(N_{no}|M_i)$, $(N_{min}|M_i)$, $(N_{mod}|M_i)$, and $(N_{maj}|M_i)$, are the number of samples with no, minor, moderate, and major liquefaction due to an M_i earthquake and N is the sample size and is equal to 81 in this study. By repeating the same process for various moment magnitudes, the liquefaction potential probability matrix can be constructed.

The liquefaction potential index P_L of each earthquake-site sample subjected to a moment magnitude 7.5 earthquake is shown in table 4-1. Following the classification shown in table 3-I, the 81 P_L values are classified into no, minor, moderate, and major liquefaction. Then, the probabilities of no, minor, moderate, and major liquefaction are calculated by using equations (4.1) through (4.4) and are listed in table 4-II. The results indicate that if a moment magnitude 7.5 earthquake occurs at Marked Tree, Arkansas, the site at President Island will have a 43.2% chance to experience major liquefaction and a 38.3% chance to experience moderate liquefaction. The chance of minor and no liquefaction at the site is 14.8% and 3.7%, respectively. By repeating the same procedure for moment magnitudes 6.5, 7.0, and 8.0, the liquefaction potential probability matrix of the site is constructed and shown in table 4-II. The mean values of the peak ground acceleration (PGA) of each moment magnitude is also shown in the table. The statistics of the peak ground acceleration are shown in table 4-III.

Table 4-I P_L Values of Earthquake-Site Samples (M = 7.5)

Sample	PBA (g)	PGA (g)	P_L	P_L (Seed)
1	0.414	0.176	7.50	8.13
2	0.464	0.191	0.22	3.92
3	0.362	0.206	0.00	0.47
4	0.379	0.183	18.80	8.45
5	0.403	0.183	8.00	3.37
6	0.401	0.197	3.71	0.00
7	0.458	0.251	20.22	18.37
8	0.474	0.225	11.06	5.78
9	0.443	0.243	7.27	2.92
10	0.249	0.148	12.71	6.57
11	0.312	0.144	1.14	0.00
12	0.261	0.165	0.00	0.00
13	0.321	0.162	15.50	7.43
14	0.302	0.154	6.03	0.92
15	0.241	0.171	3.40	0.00
16	0.264	0.177	19.30	8.18
17	0.305	0.173	10.25	2.60
18	0.243	0.170	2.89	0.00
19	0.252	0.139	11.88	5.95
20	0.237	0.136	1.74	0.00
21	0.233	0.132	0.00	0.00
22	0.261	0.161	16.36	7.34
23	0.241	0.150	7.40	0.51
24	0.242	0.156	0.67	0.00
25	0.237	0.164	17.78	7.51
26	0.253	0.166	9.04	2.04
27	0.228	0.158	3.32	0.00

Table 4-I P_L Values of Earthquake-Site Samples (M = 7.5) (Continued)

Sample	PBA (g)	PGA (g)	P_L	P_L (Seed)
28	0.524	0.195	19.31	9.01
29	0.442	0.185	6.39	3.54
30	0.495	0.205	1.92	0.39
31	0.452	0.256	25.16	18.99
32	0.511	0.246	13.62	7.91
33	0.453	0.213	9.40	0.98
34	0.440	0.253	31.02	18.71
35	0.539	0.244	19.06	7.55
36	0.509	0.235	12.60	2.41
37	0.325	0.184	18.32	8.49
38	0.380	0.176	8.62	2.82
39	0.365	0.198	4.15	0.00
40	0.341	0.199	21.91	9.73
41	0.357	0.210	14.24	5.04
42	0.388	0.182	7.17	0.00
43	0.345	0.245	33.15	17.66
44	0.403	0.210	17.07	5.05
45	0.348	0.209	12.16	0.70
46	0.278	0.150	16.04	6.70
47	0.300	0.174	7.64	2.67
48	0.263	0.160	0.95	0.00
49	0.305	0.175	22.68	8.07
50	0.291	0.193	13.71	4.03
51	0.300	0.178	9.45	0.00
52	0.273	0.198	27.60	9.63
53	0.360	0.219	16.10	5.50
54	0.287	0.195	12.30	0.00

Table 4-I P_L Values of Earthquake-Site Samples (M = 7.5) (Continued)

Sample	PBA (g)	PGA (g)	P_L	P_L (Seed)
55	0.500	0.214	19.08	12.78
56	0.526	0.213	12.00	5.22
57	0.551	0.185	4.62	0.00
58	0.596	0.235	28.82	16.13
59	0.695	0.230	17.26	6.00
60	0.582	0.242	12.80	2.86
61	0.597	0.276	38.17	21.42
62	0.732	0.233	19.74	6.16
63	0.618	0.280	16.76	4.67
64	0.462	0.195	20.07	8.93
65	0.421	0.207	12.79	4.87
66	0.408	0.185	6.01	0.00
67	0.419	0.276	27.51	21.39
68	0.548	0.210	16.70	5.03
69	0.470	0.199	12.29	0.00
70	0.430	0.214	31.86	12.67
71	0.445	0.217	18.88	5.38
72	0.408	0.225	15.71	1.85
73	0.335	0.193	20.43	8.84
74	0.347	0.179	12.41	3.08
75	0.376	0.168	6.20	0.00
76	0.413	0.190	26.91	8.76
77	0.348	0.241	17.20	7.07
78	0.352	0.186	12.02	0.00
79	0.405	0.201	32.15	10.11
80	0.363	0.223	20.43	5.72
81	0.329	0.220	13.50	1.51

Table 4-II Liquefaction Potential Probability Matrix (Proposed Method)

M	Mean PGA (g)	Probability of Liquefaction (%)			
		No	Minor	Moderate	Major
6.5	0.128	90.12	8.64	1.23	0.00
7.0	0.164	45.68	27.16	18.52	8.64
7.5	0.198	3.70	14.81	38.27	43.21
8.0	0.238	0.00	0.00	12.35	87.65

Table 4-III Statistics of Peak Ground Accelerations

M	Range (g)	Mean (g)	SD (g)	COV
6.5	0.084-0.213	0.128	0.027	0.207
7.0	0.109-0.245	0.164	0.030	0.182
7.5	0.132-0.280	0.198	0.034	0.173
8.0	0.164-0.332	0.238	0.043	0.180

4.2 Fragility Curves

The fragility curves express the probabilities that a site will have at least minor, at least moderate, and major liquefaction at various moment

magnitude earthquakes. For a specified moment magnitude M_i, these probabilities can be determined as follows:

$$F_r(\text{min}|M_i) = P(\text{min}|M_i) + P(\text{mod}|M_i) + P(\text{maj}|M_i) \quad (4.5)$$

$$F_r(\text{mod}|M_i) = P(\text{mod}|M_i) + P(\text{maj}|M_i) \quad (4.6)$$

$$F_r(\text{maj}|M_i) = P(\text{maj}|M_i) \quad (4.7)$$

where $F_r(\text{min}|M_i)$, $F_r(\text{mod}|M_i)$, and $F_r(\text{maj}|M_i)$ denote the probability that the site will have at least minor, at least moderate, and major liquefaction, respectively, if an earthquake of moment magnitude M_i occurs. From the liquefaction potential probability matrix (table 4-II), the fragility data is calculated and shown in table 4-IV. Then, the fragility curves corresponding to at least minor, at least moderate, and major liquefaction is constructed as shown in figure 4-1.

Table 4-IV Fragility Data (Proposed Method)

M	Mean PGA (g)	Probability of Liquefaction (%)		
		Minor	Moderate	Major
6.5	0.13	9.87	1.23	0.00
7.0	0.16	54.32	27.16	8.64
7.5	0.20	96.30	81.48	43.21
8.0	0.24	100.00	100.00	87.65

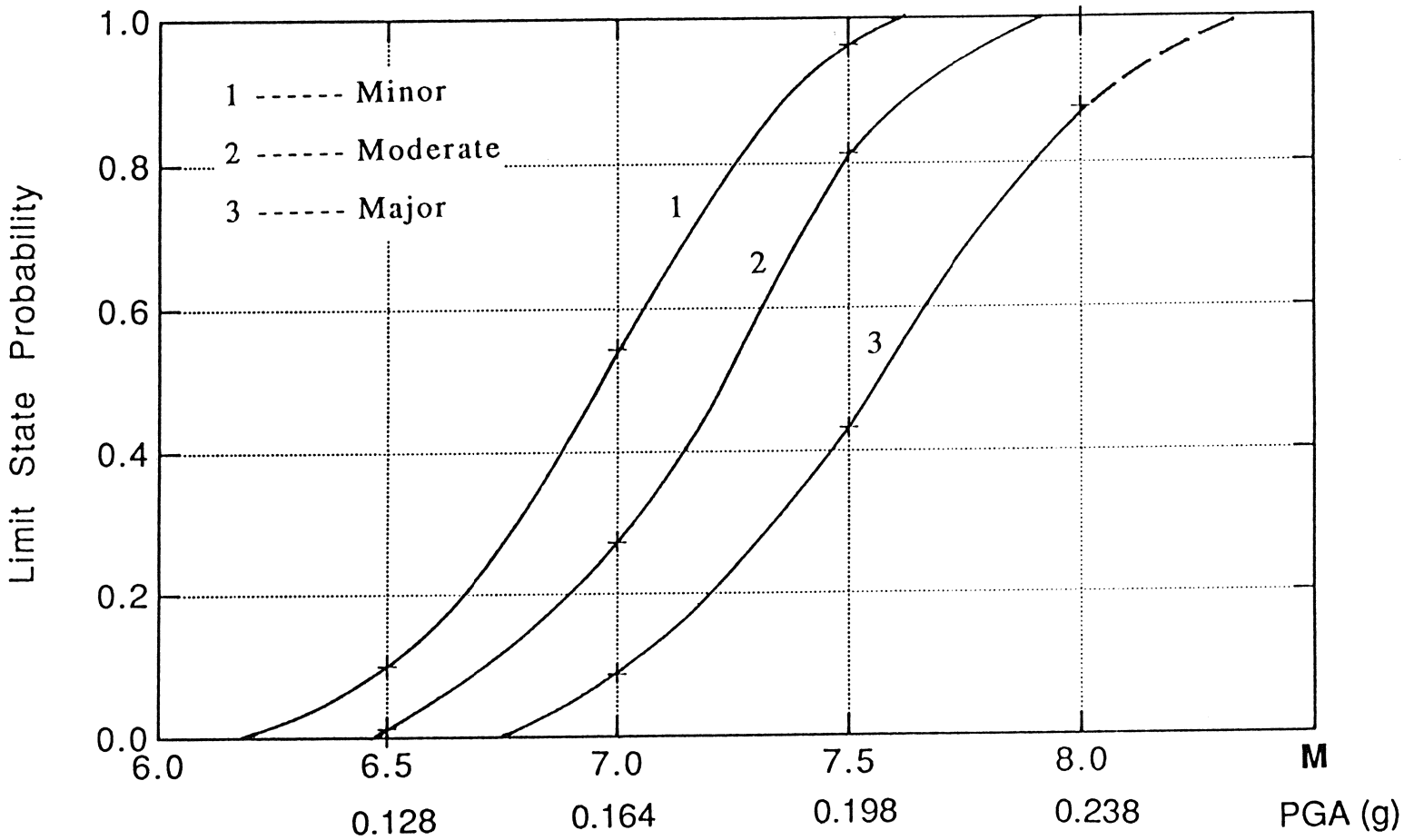

FIGURE 4-1 Fragility Curves for President Island Site (Proposed Method)

SECTION 5

COMPARISON OF RESULTS

In this section, the results obtained from the proposed method are compared with those obtained by using the simplified procedure developed by Seed and Idriss [6,7]. This simplified procedure is briefly described below.

5.1 Simplified Procedure

For the factor of safety against liquefaction F_L, the earthquake-induced shear stress ratio L is determined from the following equation.

$$L = 0.65\ a_{max}\ x\ \left(\frac{\sigma_0}{\sigma'_0}\right)\ x\ r_d \qquad (5.1)$$

where a_{max} is the peak ground acceleration in g. In this study, the peak ground accelerations shown in table 4-I are determined from nonlinear site response analysis. σ_0 and σ'_0 are the total and effective vertical confining pressure, respectively. r_d is the stress reduction factor and can be obtained from figure 5-1 [7] or from the following formula [4].

$$r_d = 1 - 0.011\ z \qquad (5.2)$$

where z is the depth in meter measured from the ground level.

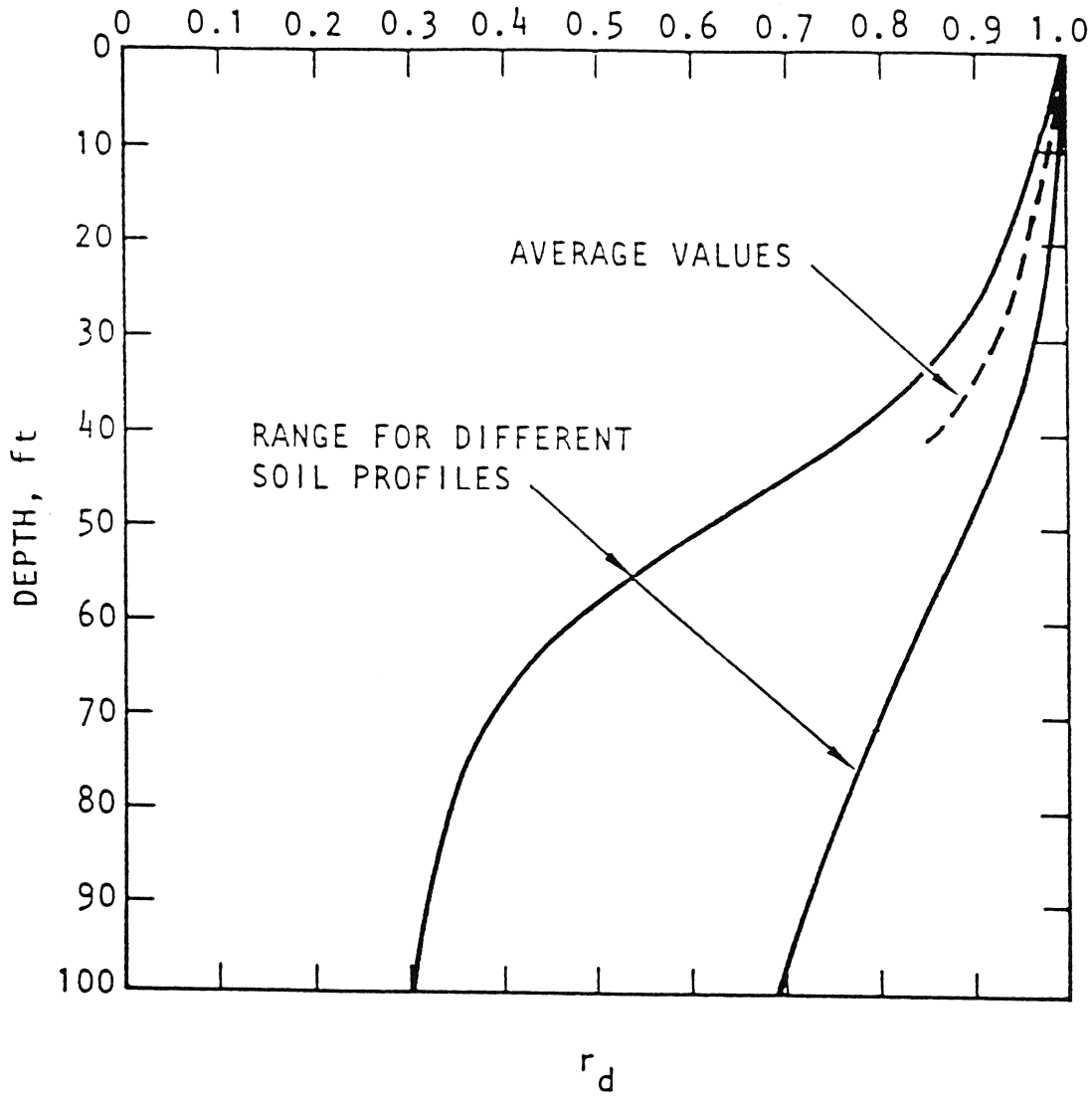

FIGURE 5-1 Range of r_d Values (after Seed and Idriss 1982)

The resistance shear stress ratio R is determined from the resistance curves (figure 5-2) for sand and silty sand on the basis of the corrected blowcount $(N_1)_{60}$. The resistance curves shown in figure 5-2 are applicable for magnitude 7.5 and are established based on actual field data from earthquakes around the world. For magnitude other than 7.5, the curves need to be multiplied by a factor (table 5-I) as suggested by Seed and Idriss [7].

Table 5-I Scaling Factor for Various Magnitudes

Magnitude	Scaling Factor
8.50	0.89
7.50	1.00
6.75	1.13
6.00	1.32
5.25	1.50

From the R and L values, the factor of safety F_L of each potentially liquefiable layer can be determined. Then, the liquefaction potential index P_L of the site is computed from equation (3.5). The 81 P_L values obtained by using the simplified procedure for an M = 7.5 earthquake are also shown in table 4-I. The liquefaction potential probability matrix and fragility curves are calculated using the same approach as the proposed method. For the selected site, the liquefaction potential probability matrix obtained by using the simplified procedure is shown in table 5-II. The

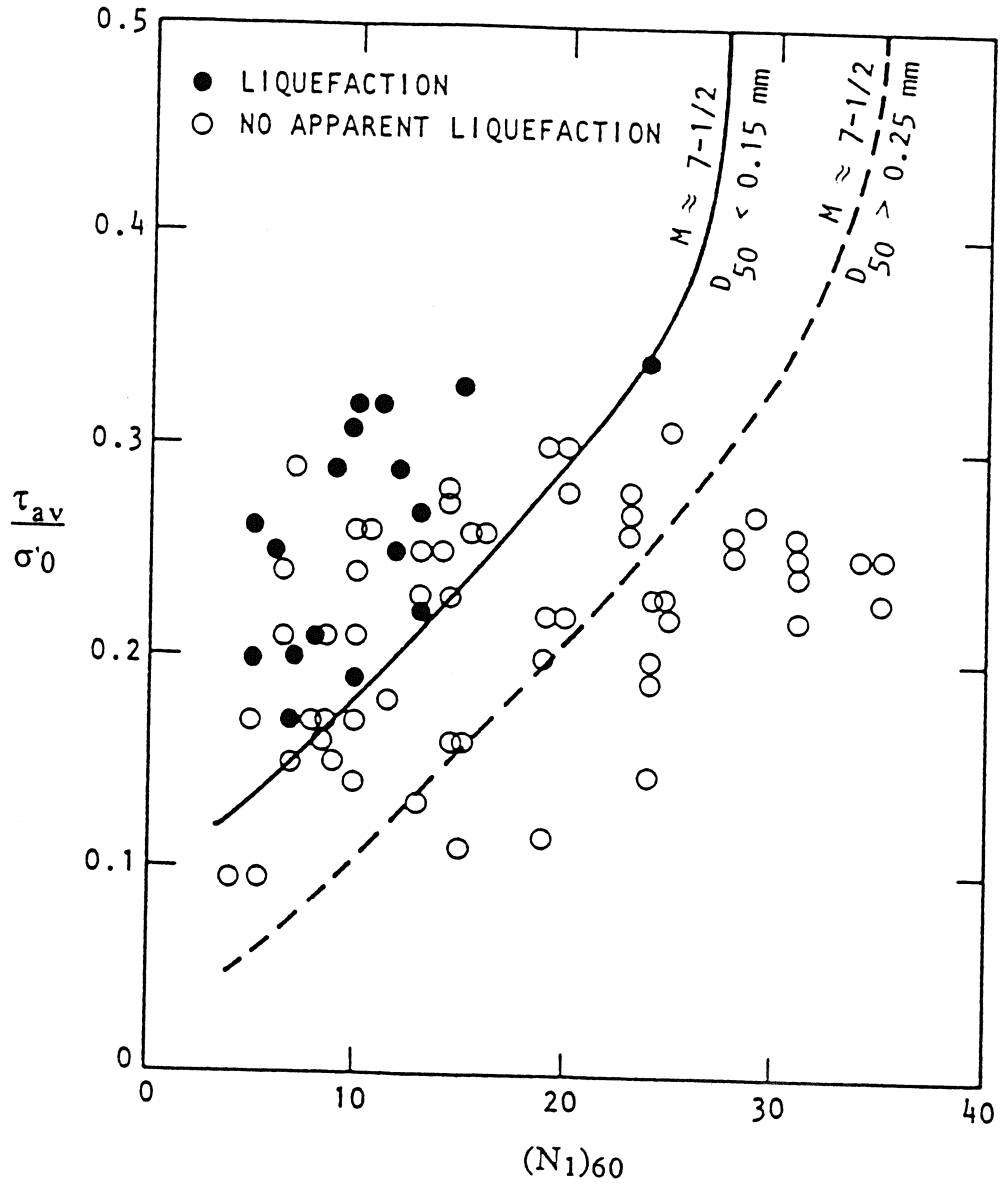

FIGURE 5-2 Liquefaction Resistance Curves for Sand and Silty Sand (after Seed and Idriss 1982)

fragility data and the corresponding fragility curves are shown in table 5-III and figure 5-3, respectively.

Table 5-II Liquefaction Potential Probability Matrix (Simplified Method)

	Probability of Liquefaction (%)			
M	No	Minor	Moderate	Major
6.5	71.60	22.22	6.17	0.00
7.0	43.21	30.86	25.93	0.00
7.5	23.46	27.16	40.74	8.64
8.0	0.00	29.63	35.80	34.57

Table 5-III Fragility Data (Simplified Method)

	Probability of Liquefaction(%)		
M	Minor	Moderate	Major
6.5	28.39	6.17	0.00
7.0	56.79	25.93	0.00
7.5	76.54	49.38	8.64
8.0	100.0	70.37	34.57

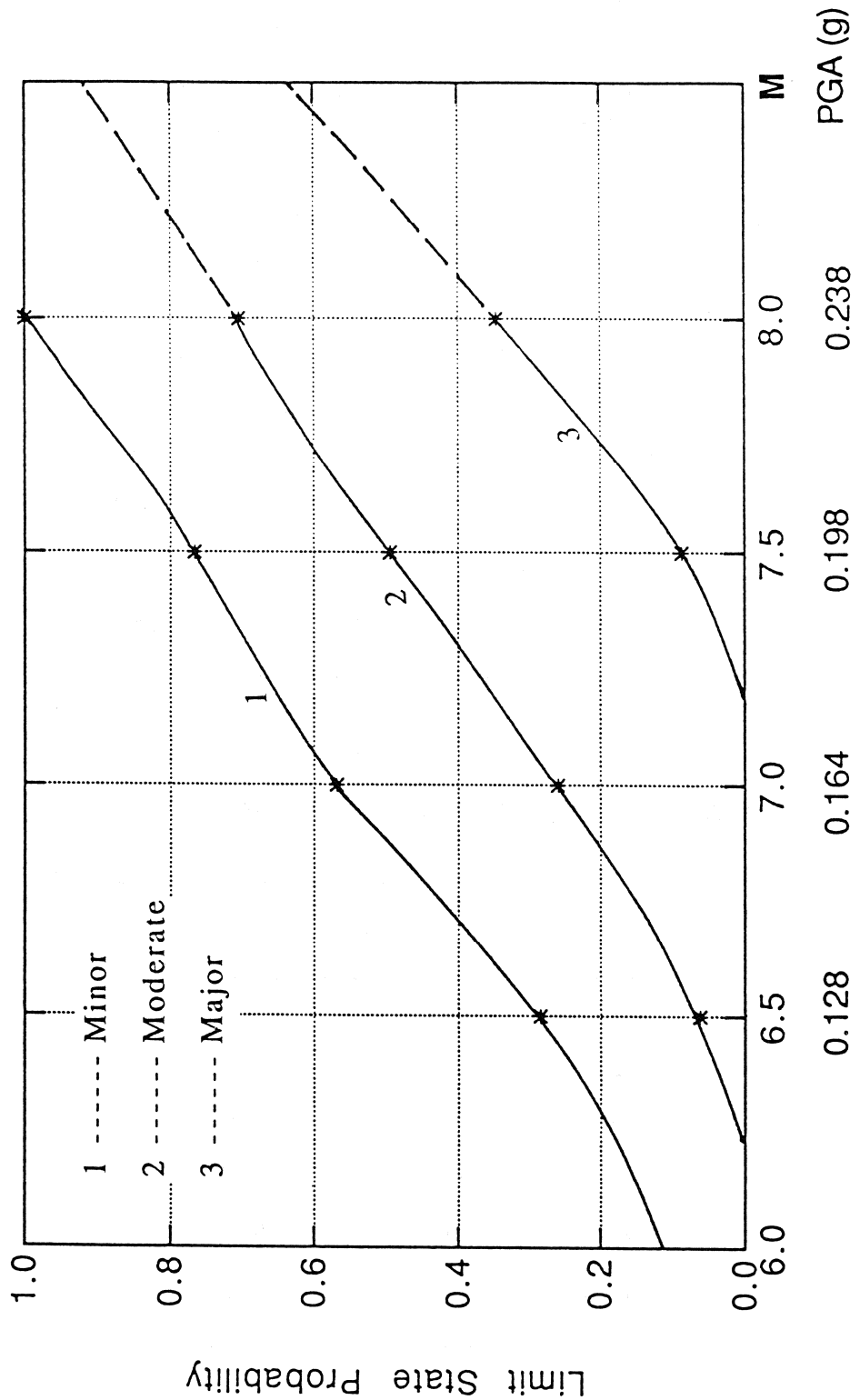

FIGURE 5-3 Fragility Curves for President Island Site (Simplified Method)

The earthquake-induced shear stress ratios L obtained from the simplified method are close to those obtained from site response analysis in the proposed method. It is noted that the peak ground acceleration used in the simplified formula is also from the results of nonlinear site response analysis. Thus, the L values computed by both methods are expected to be close. The resistance shear stress ratios R evaluated by both methods are quite different. In the proposed method, the R is computed based on the equivalent uniform cycles N_{eq}, relative density of sand D_r, and the laboratory test data, while the R value obtained by using the simplified procedure is based on the field data and corrected blowcount $(N_1)_{60}$. The equivalent uniform cycles N_{eq} as suggested by Seed and Idriss [7] in the simplified method are quite different from those obtained under New Madrid earthquakes. The difference in the equivalent uniform cycles contributes significantly to the difference in R values.

The fragility curves obtained from the proposed method (solid line) and those obtained by the simplified method (dashed line) are shown in figure 5-4. For an $\mathbf{M} = 7.0$ earthquake, the results predicted by both methods are comparable. For an $\mathbf{M} \geq 7.5$ earthquake, the chance of liquefaction evaluated by the proposed method is much larger than that obtained by the simplified method. However, the reverse is true for an $\mathbf{M} = 6.5$ earthquake.

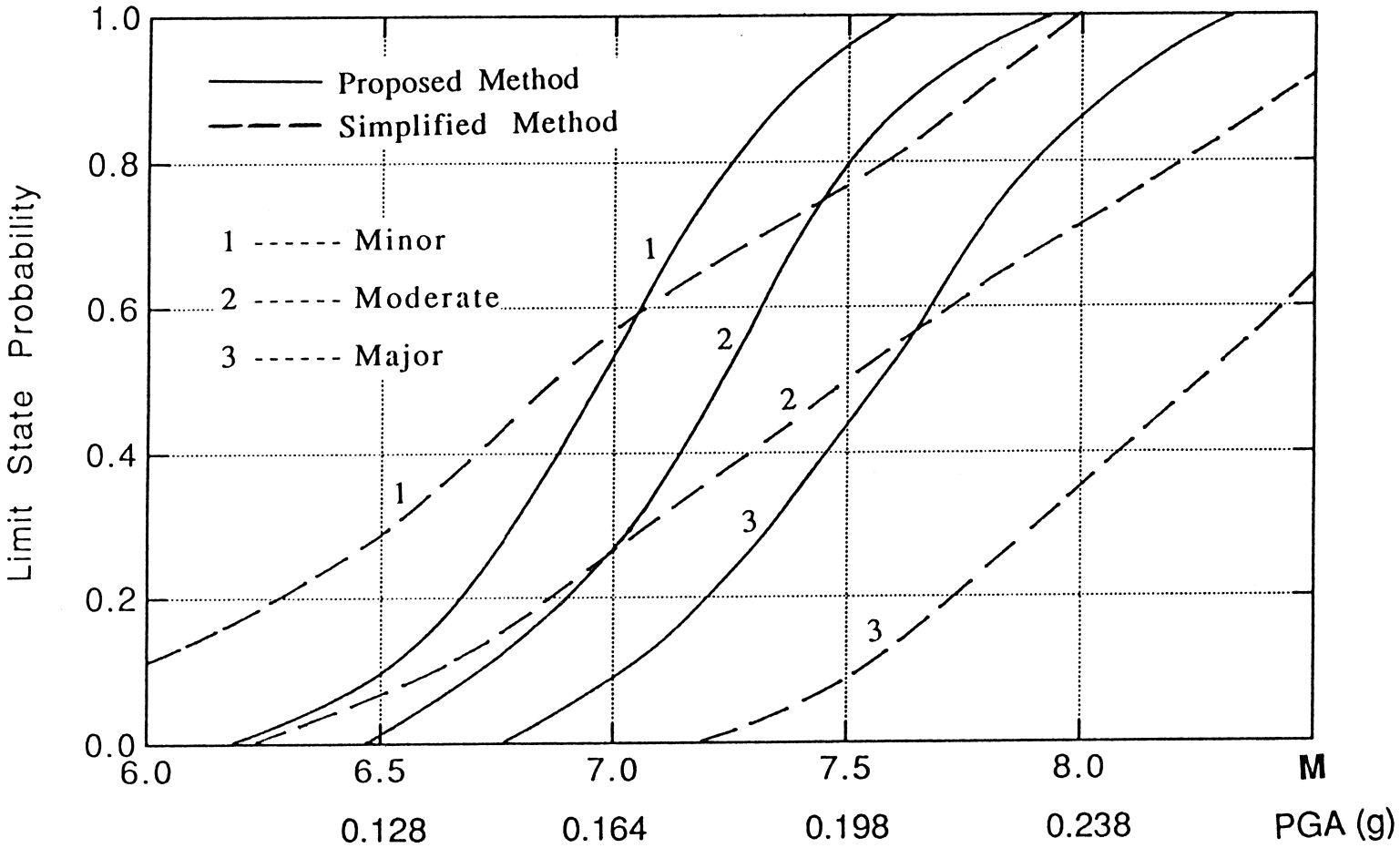

FIGURE 5-4 Comparison of Fragility Curves

SECTION 6

CONCLUSIONS

The liquefaction potential of a saturated sand site is affected by site parameters such as relative density, percentage of clay, and effective confining pressure. In addition, it is also affected by seismic parameters such as the magnitude, frequency content, and duration of an earthquake. In this study, a probabilistic approach for evaluating liquefaction potential of a site is presented and illustrated by using a site at President Island, Memphis, Tennessee, which is close to the New Madrid seismic zone. The results are presented in terms of the liquefaction potential probability matrix and fragility curves. The major conclusions are as follows:

1. The proposed method incorporates local site conditions and regional seismicity in the evaluation of the liquefaction potential of a site. In addition, uncertainties in seismic and site parameters can be easily included in the analysis. Thus, the proposed method is appropriate for evaluating the liquefaction potential of a specific site.

2. The site at President Island, Memphis, probably will not be liquefied if a moderate New Madrid earthquake (e.g., **M** = 6.5) occurs at Marked Tree, Arkansas. On the other hand, when the site is subject to a large earthquake, for example, a 7.5 moment magnitude earthquake, the probability that the site will have major liquefaction is 43%; at least moderate liquefaction is about 80%; and the site is almost certain to have at least minor liquefaction. Thus, the liquefaction potential at

President Island should be carefully evaluated if a critical facility is to be constructed there.

3. The fragility curves obtained from this study are compared with those using the simplified method proposed by Seed and Idriss [6,7]. For an **M** = 7.0 earthquake, the results predicted by both methods are comparable. For an **M** $\geq$ 7.5 earthquake, the chance of liquefaction evaluated by means of the proposed method is much larger than that obtained by means of the simplified method. However, the reverse is true for an **M** = 6.5 earthquake. The earthquake-induced shear stress predicted by using both methods are close, since both methods use the results from nonlinear site response analysis. However, the resistance shear stress ratio R evaluated by using both methods is quite different. In the proposed method, the R value is evaluated based on the equivalent uniform cycles N_{eq}, relative density of sand D_r, and the laboratory test data, while the R value obtained by using the simplified method is based on the field data and corrected blowcount $(N_1)_{60}$. The equivalent uniform cycles N_{eq} as suggested by Seed and Idriss [7] in the simplified method are quite different from those obtained from the proposed method for New Madrid earthquakes. This contributes significantly to the difference in both methods.

In the proposed method for evaluating liquefaction potential of a site, the resistance shear stress ratio R is evaluated based on laboratory test data. However, tests performed on reconstituted samples with identical values of D_r have shown a tremendous sensitivity to, among other factors, the exact method of sample preparation. Since test results may have large

variation unless use of undisturbed soil samples, the resistance shear stress ratio R will be established by other means in the future. For example, the R value may be obtained from field data. Furthermore, the nonlinear site response is obtained by performing the MASH computer code in this study. Since various codes for nonlinear site response do not usually give identical results for the same problem. Other computer codes such as SHAKE and DYNA1D will also be used in the future to compare the results of nonlinear site response analysis.

The proposed method is appropriate for evaluating the liquefaction potential of a specific site; however, it may be too cumbersome for evaluating liquefaction potential of a region. Further study is needed to develop a method that is applicable to a region.

SECTION 7

REFERENCES

1. Seed, H.B., and Idriss, I.M., "Analysis of Soil Liquefaction: Niigata Earthquake," Journal of the Soil Mechanics and Foundations Division, ASCE, Vol. 93, No. SM3, May, 1967, pp. 83-108.

2. Ishihara, K., and Koga, Y., "Case Studies of Liquefaction in the 1964 Niigata Earthquake," Soils and Foundations, Japanese Society of Soil Mechanics and Foundation Engineering, Vol. 21, No. 3, September, 1981, pp. 35-52.

3. Seed, H.B., Idriss, I.M., Makdisi, F., and Banerjee, N., "Representation of Irregular Stress Time Histories by Equivalent Uniform Stress Series in Liquefaction Analyses," EERC 75-29, Earthquake Engineering Research Center, University of California, Berkeley, October, 1975.

4. Iwasaki, T., Tokida, K., Tatsuoka, F., Watanabe, S., Yasuda, S., Sato, H., "Microzonation for Soil Liquefaction Potential Using Simplified Methods," Proceedings of the 3rd International Earthquake Microzonation Conference, Seattle, 1982.

5. Okumura, T., and Shinozuka, M., "Seismic Hazard Analysis for Assessment of Liquefaction Potential," Proceedings of the Fourth U.S. National Conference on Earthquake Engineering, Palm Springs, Ca, May 20-24, Vol. 1, 1990, pp. 771-780.

6. Seed, H.B., and Idriss, I.M., "Simplified Procedure for Evaluating Soil Liquefaction Potential," Journal of the Soil Mechanics and Foundations Division, ASCE, Vol. 97, No. SM9, September, 1971, pp. 1249-1273.

7. Seed, H.B., and Idriss, I.M., "Ground Motions and Soil Liquefaction During Earthquakes," Earthquake Engineering Research Institue (EERI), Pasadena, California, December, 1982.

8. Martin, P.P., and Seed, H.B., "MASH, A Computer Program for the Non-linear Analysis of Vertically Propagating Shear Waves in Horizontally Layered Deposits," Report No. UCB/EERC-78/23, Earthquake Engineering Research Center, University of California, Berkeley, California, October, 1978.

9. Tokimatsu K., and Seed, H.B., "Evaluation of Settlement in Sands due to Earthquake Shaking," Journal of Geotechnical Engineering Division, ASCE, Vol. 113, No. 8, August, 1986, pp. 861-895.

10. Seed, H.B., Tokimatsu, K., Harder, L.F., Chung, R.M., "Influence of SPT Procedures in Soil Liquefaction Resistance Evaluations," Journal of the Soil Mechanics and Foundations Division, ASCE, Vol. 111, No. 12, December, 1985, pp. 1425-1445.

11. Seed, H.B., and Idriss, I.M., "Soil Moduli and Damping Factors for Dynamic Response Analysis", Report No. EERC 70-10, University of California, Berkeley, December, 1970.

12. Shibata, T., and Soelarno, D.S., "Stress Strain Characteristics of Sands Under Cyclic Loading," Proceedings of Japanese Society of Civil Engineering, Vol. 239, 1975, pp. 57-65.

13. Iwasaki, T., Tatsuoka, F., and Takagi, Y., "Dynamic Shear Deformation Properties of Sand for Wide Strain Range," Report of Civil Engineering Institution, No. 1085, Ministry of Construction, Tokyo, Japan, 1976.

14. Seed, H.B., Wong, R.T., Idriss, I.M., and Tokimatsu, K., "Moduli and Damping Factors for Dynamic Analyses of Cohesionless Soils," Journal of the Geotechnical Engineering Division, ASCE, Vol. 112, No. 11, November, 1986, pp. 1016-1032.

15. Hardin, B.O., and Drnevich, V.P., "Shear Modulus and Damping in Soils: Design Equations and Curves," Journal of the Soil Mechanics and Foundations Division, ASCE, Vol. 98, No. SM7, July, 1972, pp. 667-692.

16. Hwang, H., and Lee, C.S., "Parametric Study of Site Response Analysis," Accepted for publication in the International Journal of Soil Dynamics and Earthquake Engineering, 1991.

17. Zen, K., Umehara, Y., and Hamada, K., "Laboratory Tests and In-Situ Seismic Survey on Vibratory Shear Modulus of Clayey Soils with Various Plasticities," Proceedings of Fifth Japan Earthquake Engineering Symposium, Tokyo, Japan, November, 1978, pp. 721-728.

18. Dobry, R., and Vucetic, M., "Dynamic Properties and Seismic Response of Soft Clay Deposits," Proceedings of International Symposium on Geotechnical Engineering of Soft Soils, Vol. 2, Mexico City, Mexico, August, 1987, pp. 51-87.

19. Sun, J.I., Golesorkhi, R., and Seed, H.B., "Dynamic Moduli and Damping Ratios for Cohesive Soils," Report No. UCB/EERC-88/15, Earthquake Engineering Research Center, University of California, Berkeley, California, August, 1988.

20. Hanks, T.C., and McGuire, R.K., "The Character of High Frequency Strong Ground Motion," Bulletin of Seismic Society of America, Vol. 71, 1981, pp. 2071-2095.

21. Boore, D.M., and Atkinson, G.M., "Stochastic Prediction of Ground Motion and Spectral Response Parameters at Hard-Rock Sites in Eastern North America," Bulletin of the Seismological Society of America, Vol. 77, No. 2, April, 1987, pp. 440-467.

22. Boore, D.M., "The Prediction of Strong Ground Motion," in Erdik, M.O., and Toksoz, M.N., Editors, Strong Ground Motion Seismology, D. Reidel Publishing Company, Boston, MA, 1987, pp. 109-141.

23. Brune, J.N., "Tectonic Stress and Spectra of Seismic Shear Waves from Earthquakes," Journal of Geophysical Research, Vol. 75, No. 26, September, 1970, pp. 4997-5009.

24. Boore, D.M., and Boatwright J., "Average Body-Wave Radiation Coefficients," Bulletin of the Seismological Society of America, Vol. 74, No. 5, October, 1984, pp. 1615-1621.

25. Dwyer, J.J., Herrmann, R.B., and Nuttli, O.W., "Spatial Attenuation of the Lg Wave in the Central United States," Bulletin of the Seismological Society of America, Vol. 73, No. 3, June, 1983, pp. 781-796.

26. Jacob, K., Hough S., Fribeng P., and Gaviel, J.C., Unpublished Workshop Notes, 1990.

27. Shinozuka, M., "Digital Simulation of Random Processes in Engineering Mechanics with the Aid of FFT Technique," in Ariaratnam, S.T., and Leipholz, H.H.E., eds., Stochastic Problems in Mechanics, University of Waterloo Press, Waterloo, 1974, pp. 277-286.

28. Hwang, H., Chen, C.H., and Yu, G., "Bedrock Accelerations in Memphis Area due to Large New Madrid Earthquakes," Technical Report NCEER-89-0029, National Center for Earthquake Engineering Research, SUNY, Buffalo, NY, November, 1989.

29. McGuire, R.K., Toro, G.R., and Silva, W.J., "Engineering Model of Earthquake Ground Motion for Eastern North America," Risk Engineering, Inc., EPRI NP-6074, October, 1988.

30. Atkinson, G.M., and Boore, D.M., "Preliminary Analysis of Ground Motion Data from the 25 November 1988 Saguenay, Quebec, Earthquake," Seismological Society of America, Abstract of 84th Annual Meeting, 1989.

31. Hanks, T.C., "b-values and $\omega^{-\gamma}$ Seismic Source Models: Implications for Tectonic Stress Variations Along Active Crustal Fault Zones and the Estimation of High-Frequency Strong Ground Motion," Journal of Geophysical Research, Vol. 84, 1979, pp. 2235-2242.

32. Johnston, A.C., "Seismic Ground Motions in Shelby County, Tennessee, Resulting from Large New Madrid Earthquakes," Technical Report of Center for Earthquake Research and Information, Memphis State University, January, 1988.

33. Krinitzsky, E.L., Chang, F.K., and Nuttli, O.W., "Magnitude-Related Earthquake Ground Motions," Bulletin of the Association of Engineering Geologists, Vol. XXV, No. 4, 1988, pp. 399-423.

34. Lai, P.S.-S., "Statistical Characterization of Strong Ground Motions Using Power Spectral Density Functions," Bulletin of the Seismological Society of America, Vol. 72, No. 1, 1982, pp. 259-274.

35. Seed, H.B., and Peacock, W.H., "Test Procedures for Measuring Soil Liquefaction Characteristics," Journal of the Soil Mechanics and Foundations Division, ASCE, Vol. 97, No. SM8, August, 1971, pp. 1099-1119.

36. Ueng, T.S., and Chang, C.S., "The Effect of Clay Contents on Liquefaction of Fulung Sand," Proceedings of the Seventh Southeast Asian Geotechnical Conference, November, 1982.

37. Chang, T.S., Tang, P.S., Lee, C.S., and Hwang, H., "Evaluation of Liquefaction Potential in Memphis and Shelby County," Technical Report NCEER-90-0018, National Center for Earthquake Engineering Research, SUNY, Buffalo, NY, August, 1990.

NATIONAL CENTER FOR EARTHQUAKE ENGINEERING RESEARCH
LIST OF TECHNICAL REPORTS

The National Center for Earthquake Engineering Research (NCEER) publishes technical reports on a variety of subjects related to earthquake engineering written by authors funded through NCEER. These reports are available from both NCEER's Publications Department and the National Technical Information Service (NTIS). Requests for reports should be directed to the Publications Department, National Center for Earthquake Engineering Research, State University of New York at Buffalo, Red Jacket Quadrangle, Buffalo, New York 14261. Reports can also be requested through NTIS, 5285 Port Royal Road, Springfield, Virginia 22161. NTIS accession numbers are shown in parenthesis, if available.

NCEER-87-0001 "First-Year Program in Research, Education and Technology Transfer," 3/5/87, (PB88-134275/AS).

NCEER-87-0002 "Experimental Evaluation of Instantaneous Optimal Algorithms for Structural Control," by R.C. Lin, T.T. Soong and A.M. Reinhorn, 4/20/87, (PB88-134341/AS).

NCEER-87-0003 "Experimentation Using the Earthquake Simulation Facilities at University at Buffalo," by A.M. Reinhorn and R.L. Ketter, to be published.

NCEER-87-0004 "The System Characteristics and Performance of a Shaking Table," by J.S. Hwang, K.C. Chang and G.C. Lee, 6/1/87, (PB88-134259/AS). This report is available only through NTIS (see address given above).

NCEER-87-0005 "A Finite Element Formulation for Nonlinear Viscoplastic Material Using a Q Model," by O. Gyebi and G. Dasgupta, 11/2/87, (PB88-213764/AS).

NCEER-87-0006 "Symbolic Manipulation Program (SMP) - Algebraic Codes for Two and Three Dimensional Finite Element Formulations," by X. Lee and G. Dasgupta, 11/9/87, (PB88-219522/AS).

NCEER-87-0007 "Instantaneous Optimal Control Laws for Tall Buildings Under Seismic Excitations," by J.N. Yang, A. Akbarpour and P. Ghaemmaghami, 6/10/87, (PB88-134333/AS).

NCEER-87-0008 "IDARC: Inelastic Damage Analysis of Reinforced Concrete Frame - Shear-Wall Structures," by Y.J. Park, A.M. Reinhorn and S.K. Kunnath, 7/20/87, (PB88-134325/AS).

NCEER-87-0009 "Liquefaction Potential for New York State: A Preliminary Report on Sites in Manhattan and Buffalo," by M. Budhu, V. Vijayakumar, R.F. Giese and L. Baumgras, 8/31/87, (PB88-163704/AS). This report is available only through NTIS (see address given above).

NCEER-87-0010 "Vertical and Torsional Vibration of Foundations in Inhomogeneous Media," by A.S. Veletsos and K.W. Dotson, 6/1/87, (PB88-134291/AS).

NCEER-87-0011 "Seismic Probabilistic Risk Assessment and Seismic Margins Studies for Nuclear Power Plants," by Howard H.M. Hwang, 6/15/87, (PB88-134267/AS).

NCEER-87-0012 "Parametric Studies of Frequency Response of Secondary Systems Under Ground-Acceleration Excitations," by Y. Yong and Y.K. Lin, 6/10/87, (PB88-134309/AS).

NCEER-87-0013 "Frequency Response of Secondary Systems Under Seismic Excitation," by J.A. HoLung, J. Cai and Y.K. Lin, 7/31/87, (PB88-134317/AS).

NCEER-87-0014 "Modelling Earthquake Ground Motions in Seismically Active Regions Using Parametric Time Series Methods," by G.W. Ellis and A.S. Cakmak, 8/25/87, (PB88-134283/AS).

NCEER-87-0015 "Detection and Assessment of Seismic Structural Damage," by E. DiPasquale and A.S. Cakmak, 8/25/87, (PB88-163712/AS).

NCEER-87-0016 "Pipeline Experiment at Parkfield, California," by J. Isenberg and E. Richardson, 9/15/87, (PB88-163720/AS). This report is available only through NTIS (see address given above).

NCEER-87-0017 "Digital Simulation of Seismic Ground Motion," by M. Shinozuka, G. Deodatis and T. Harada, 8/31/87, (PB88-155197/AS). This report is available only through NTIS (see address given above).

NCEER-87-0018 "Practical Considerations for Structural Control: System Uncertainty, System Time Delay and Truncation of Small Control Forces," J.N. Yang and A. Akbarpour, 8/10/87, (PB88-163738/AS).

NCEER-87-0019 "Modal Analysis of Nonclassically Damped Structural Systems Using Canonical Transformation," by J.N. Yang, S. Sarkani and F.X. Long, 9/27/87, (PB88-187851/AS).

NCEER-87-0020 "A Nonstationary Solution in Random Vibration Theory," by J.R. Red-Horse and P.D. Spanos, 11/3/87, (PB88-163746/AS).

NCEER-87-0021 "Horizontal Impedances for Radially Inhomogeneous Viscoelastic Soil Layers," by A.S. Veletsos and K.W. Dotson, 10/15/87, (PB88-150859/AS).

NCEER-87-0022 "Seismic Damage Assessment of Reinforced Concrete Members," by Y.S. Chung, C. Meyer and M. Shinozuka, 10/9/87, (PB88-150867/AS). This report is available only through NTIS (see address given above).

NCEER-87-0023 "Active Structural Control in Civil Engineering," by T.T. Soong, 11/11/87, (PB88-187778/AS).

NCEER-87-0024 Vertical and Torsional Impedances for Radially Inhomogeneous Viscoelastic Soil Layers," by K.W. Dotson and A.S. Veletsos, 12/87, (PB88-187786/AS).

NCEER-87-0025 "Proceedings from the Symposium on Seismic Hazards, Ground Motions, Soil-Liquefaction and Engineering Practice in Eastern North America," October 20-22, 1987, edited by K.H. Jacob, 12/87, (PB88-188115/AS).

NCEER-87-0026 "Report on the Whittier-Narrows, California, Earthquake of October 1, 1987," by J. Pantelic and A. Reinhorn, 11/87, (PB88-187752/AS). This report is available only through NTIS (see address given above).

NCEER-87-0027 "Design of a Modular Program for Transient Nonlinear Analysis of Large 3-D Building Structures," by S. Srivastav and J.F. Abel, 12/30/87, (PB88-187950/AS).

NCEER-87-0028 "Second-Year Program in Research, Education and Technology Transfer," 3/8/88, (PB88-219480/AS).

NCEER-88-0001 "Workshop on Seismic Computer Analysis and Design of Buildings With Interactive Graphics," by W. McGuire, J.F. Abel and C.H. Conley, 1/18/88, (PB88-187760/AS).

NCEER-88-0002 "Optimal Control of Nonlinear Flexible Structures," by J.N. Yang, F.X. Long and D. Wong, 1/22/88, (PB88-213772/AS).

NCEER-88-0003 "Substructuring Techniques in the Time Domain for Primary-Secondary Structural Systems," by G.D. Manolis and G. Juhn, 2/10/88, (PB88-213780/AS).

NCEER-88-0004 "Iterative Seismic Analysis of Primary-Secondary Systems," by A. Singhal, L.D. Lutes and P.D. Spanos, 2/23/88, (PB88-213798/AS).

NCEER-88-0005 "Stochastic Finite Element Expansion for Random Media," by P.D. Spanos and R. Ghanem, 3/14/88, (PB88-213806/AS).

NCEER-88-0006 "Combining Structural Optimization and Structural Control," by F.Y. Cheng and C.P. Pantelides, 1/10/88, (PB88-213814/AS).

NCEER-88-0007 "Seismic Performance Assessment of Code-Designed Structures," by H.H-M. Hwang, J-W. Jaw and H-J. Shau, 3/20/88, (PB88-219423/AS).

NCEER-88-0008 "Reliability Analysis of Code-Designed Structures Under Natural Hazards," by H.H-M. Hwang, H. Ushiba and M. Shinozuka, 2/29/88, (PB88-229471/AS).

NCEER-88-0009 "Seismic Fragility Analysis of Shear Wall Structures," by J-W Jaw and H.H-M. Hwang, 4/30/88, (PB89-102867/AS).

NCEER-88-0010 "Base Isolation of a Multi-Story Building Under a Harmonic Ground Motion - A Comparison of Performances of Various Systems," by F-G Fan, G. Ahmadi and I.G. Tadjbakhsh, 5/18/88, (PB89-122238/AS).

NCEER-88-0011 "Seismic Floor Response Spectra for a Combined System by Green's Functions," by F.M. Lavelle, L.A. Bergman and P.D. Spanos, 5/1/88, (PB89-102875/AS).

NCEER-88-0012 "A New Solution Technique for Randomly Excited Hysteretic Structures," by G.Q. Cai and Y.K. Lin, 5/16/88, (PB89-102883/AS).

NCEER-88-0013 "A Study of Radiation Damping and Soil-Structure Interaction Effects in the Centrifuge," by K. Weissman, supervised by J.H. Prevost, 5/24/88, (PB89-144703/AS).

NCEER-88-0014 "Parameter Identification and Implementation of a Kinematic Plasticity Model for Frictional Soils," by J.H. Prevost and D.V. Griffiths, to be published.

NCEER-88-0015 "Two- and Three- Dimensional Dynamic Finite Element Analyses of the Long Valley Dam," by D.V. Griffiths and J.H. Prevost, 6/17/88, (PB89-144711/AS).

NCEER-88-0016 "Damage Assessment of Reinforced Concrete Structures in Eastern United States," by A.M. Reinhorn, M.J. Seidel, S.K. Kunnath and Y.J. Park, 6/15/88, (PB89-122220/AS).

NCEER-88-0017 "Dynamic Compliance of Vertically Loaded Strip Foundations in Multilayered Viscoelastic Soils," by S. Ahmad and A.S.M. Israil, 6/17/88, (PB89-102891/AS).

NCEER-88-0018 "An Experimental Study of Seismic Structural Response With Added Viscoelastic Dampers," by R.C. Lin, Z. Liang, T.T. Soong and R.H. Zhang, 6/30/88, (PB89-122212/AS).

NCEER-88-0019 "Experimental Investigation of Primary - Secondary System Interaction," by G.D. Manolis, G. Juhn and A.M. Reinhorn, 5/27/88, (PB89-122204/AS).

NCEER-88-0020 "A Response Spectrum Approach For Analysis of Nonclassically Damped Structures," by J.N. Yang, S. Sarkani and F.X. Long, 4/22/88, (PB89-102909/AS).

NCEER-88-0021 "Seismic Interaction of Structures and Soils: Stochastic Approach," by A.S. Veletsos and A.M. Prasad, 7/21/88, (PB89-122196/AS).

NCEER-88-0022 "Identification of the Serviceability Limit State and Detection of Seismic Structural Damage," by E. DiPasquale and A.S. Cakmak, 6/15/88, (PB89-122188/AS).

NCEER-88-0023 "Multi-Hazard Risk Analysis: Case of a Simple Offshore Structure," by B.K. Bhartia and E.H. Vanmarcke, 7/21/88, (PB89-145213/AS).

NCEER-88-0024 "Automated Seismic Design of Reinforced Concrete Buildings," by Y.S. Chung, C. Meyer and M. Shinozuka, 7/5/88, (PB89-122170/AS).

NCEER-88-0025 "Experimental Study of Active Control of MDOF Structures Under Seismic Excitations," by L.L. Chung, R.C. Lin, T.T. Soong and A.M. Reinhorn, 7/10/88, (PB89-122600/AS).

NCEER-88-0026 "Earthquake Simulation Tests of a Low-Rise Metal Structure," by J.S. Hwang, K.C. Chang, G.C. Lee and R.L. Ketter, 8/1/88, (PB89-102917/AS).

NCEER-88-0027 "Systems Study of Urban Response and Reconstruction Due to Catastrophic Earthquakes," by F. Kozin and H.K. Zhou, 9/22/88, (PB90-162348/AS).

NCEER-88-0028 "Seismic Fragility Analysis of Plane Frame Structures," by H.H-M. Hwang and Y.K. Low, 7/31/88, (PB89-131445/AS).

NCEER-88-0029 "Response Analysis of Stochastic Structures," by A. Kardara, C. Bucher and M. Shinozuka, 9/22/88, (PB89-174429/AS).

NCEER-88-0030 "Nonnormal Accelerations Due to Yielding in a Primary Structure," by D.C.K. Chen and L.D. Lutes, 9/19/88, (PB89-131437/AS).

NCEER-88-0031 "Design Approaches for Soil-Structure Interaction," by A.S. Veletsos, A.M. Prasad and Y. Tang, 12/30/88, (PB89-174437/AS).

NCEER-88-0032 "A Re-evaluation of Design Spectra for Seismic Damage Control," by C.J. Turkstra and A.G. Tallin, 11/7/88, (PB89-145221/AS).

NCEER-88-0033 "The Behavior and Design of Noncontact Lap Splices Subjected to Repeated Inelastic Tensile Loading," by V.E. Sagan, P. Gergely and R.N. White, 12/8/88, (PB89-163737/AS).

NCEER-88-0034 "Seismic Response of Pile Foundations," by S.M. Mamoon, P.K. Banerjee and S. Ahmad, 11/1/88, (PB89-145239/AS).

NCEER-88-0035 "Modeling of R/C Building Structures With Flexible Floor Diaphragms (IDARC2)," by A.M. Reinhorn, S.K. Kunnath and N. Panahshahi, 9/7/88, (PB89-207153/AS).

NCEER-88-0036 "Solution of the Dam-Reservoir Interaction Problem Using a Combination of FEM, BEM with Particular Integrals, Modal Analysis, and Substructuring," by C-S. Tsai, G.C. Lee and R.L. Ketter, 12/31/88, (PB89-207146/AS).

NCEER-88-0037 "Optimal Placement of Actuators for Structural Control," by F.Y. Cheng and C.P. Pantelides, 8/15/88, (PB89-162846/AS).

NCEER-88-0038 "Teflon Bearings in Aseismic Base Isolation: Experimental Studies and Mathematical Modeling," by A. Mokha, M.C. Constantinou and A.M. Reinhorn, 12/5/88, (PB89-218457/AS).

NCEER-88-0039 "Seismic Behavior of Flat Slab High-Rise Buildings in the New York City Area," by P. Weidlinger and M. Ettouney, 10/15/88, (PB90-145681/AS).

NCEER-88-0040 "Evaluation of the Earthquake Resistance of Existing Buildings in New York City," by P. Weidlinger and M. Ettouney, 10/15/88, to be published.

NCEER-88-0041 "Small-Scale Modeling Techniques for Reinforced Concrete Structures Subjected to Seismic Loads," by W. Kim, A. El-Attar and R.N. White, 11/22/88, (PB89-189625/AS).

NCEER-88-0042 "Modeling Strong Ground Motion from Multiple Event Earthquakes," by G.W. Ellis and A.S. Cakmak, 10/15/88, (PB89-174445/AS).

NCEER-88-0043 "Nonstationary Models of Seismic Ground Acceleration," by M. Grigoriu, S.E. Ruiz and E. Rosenblueth, 7/15/88, (PB89-189617/AS).

NCEER-88-0044 "SARCF User's Guide: Seismic Analysis of Reinforced Concrete Frames," by Y.S. Chung, C. Meyer and M. Shinozuka, 11/9/88, (PB89-174452/AS).

NCEER-88-0045 "First Expert Panel Meeting on Disaster Research and Planning," edited by J. Pantelic and J. Stoyle, 9/15/88, (PB89-174460/AS).

NCEER-88-0046 "Preliminary Studies of the Effect of Degrading Infill Walls on the Nonlinear Seismic Response of Steel Frames," by C.Z. Chrysostomou, P. Gergely and J.F. Abel, 12/19/88, (PB89-208383/AS).

NCEER-88-0047 "Reinforced Concrete Frame Component Testing Facility - Design, Construction, Instrumentation and Operation," by S.P. Pessiki, C. Conley, T. Bond, P. Gergely and R.N. White, 12/16/88, (PB89-174478/AS).

NCEER-89-0001 "Effects of Protective Cushion and Soil Compliancy on the Response of Equipment Within a Seismically Excited Building," by J.A. HoLung, 2/16/89, (PB89-207179/AS).

NCEER-89-0002 "Statistical Evaluation of Response Modification Factors for Reinforced Concrete Structures," by H.H-M. Hwang and J-W. Jaw, 2/17/89, (PB89-207187/AS).

NCEER-89-0003 "Hysteretic Columns Under Random Excitation," by G-Q. Cai and Y.K. Lin, 1/9/89, (PB89-196513/AS).

NCEER-89-0004 "Experimental Study of 'Elephant Foot Bulge' Instability of Thin-Walled Metal Tanks," by Z-H. Jia and R.L. Ketter, 2/22/89, (PB89-207195/AS).

NCEER-89-0005 "Experiment on Performance of Buried Pipelines Across San Andreas Fault," by J. Isenberg, E. Richardson and T.D. O'Rourke, 3/10/89, (PB89-218440/AS).

NCEER-89-0006 "A Knowledge-Based Approach to Structural Design of Earthquake-Resistant Buildings," by M. Subramani, P. Gergely, C.H. Conley, J.F. Abel and A.H. Zaghw, 1/15/89, (PB89-218465/AS).

NCEER-89-0007 "Liquefaction Hazards and Their Effects on Buried Pipelines," by T.D. O'Rourke and P.A. Lane, 2/1/89, (PB89-218481).

NCEER-89-0008 "Fundamentals of System Identification in Structural Dynamics," by H. Imai, C-B. Yun, O. Maruyama and M. Shinozuka, 1/26/89, (PB89-207211/AS).

NCEER-89-0009 "Effects of the 1985 Michoacan Earthquake on Water Systems and Other Buried Lifelines in Mexico," by A.G. Ayala and M.J. O'Rourke, 3/8/89, (PB89-207229/AS).

NCEER-89-R010 "NCEER Bibliography of Earthquake Education Materials," by K.E.K. Ross, Second Revision, 9/1/89, (PB90-125352/AS).

NCEER-89-0011 "Inelastic Three-Dimensional Response Analysis of Reinforced Concrete Building Structures (IDARC-3D), Part I - Modeling," by S.K. Kunnath and A.M. Reinhorn, 4/17/89, (PB90-114612/AS).

NCEER-89-0012 "Recommended Modifications to ATC-14," by C.D. Poland and J.O. Malley, 4/12/89, (PB90-108648/AS).

NCEER-89-0013 "Repair and Strengthening of Beam-to-Column Connections Subjected to Earthquake Loading," by M. Corazao and A.J. Durrani, 2/28/89, (PB90-109885/AS).

NCEER-89-0014 "Program EXKAL2 for Identification of Structural Dynamic Systems," by O. Maruyama, C-B. Yun, M. Hoshiya and M. Shinozuka, 5/19/89, (PB90-109877/AS).

NCEER-89-0015 "Response of Frames With Bolted Semi-Rigid Connections, Part I - Experimental Study and Analytical Predictions," by P.J. DiCorso, A.M. Reinhorn, J.R. Dickerson, J.B. Radziminski and W.L. Harper, 6/1/89, to be published.

NCEER-89-0016 "ARMA Monte Carlo Simulation in Probabilistic Structural Analysis," by P.D. Spanos and M.P. Mignolet, 7/10/89, (PB90-109893/AS).

NCEER-89-P017 "Preliminary Proceedings from the Conference on Disaster Preparedness - The Place of Earthquake Education in Our Schools," Edited by K.E.K. Ross, 6/23/89.

NCEER-89-0017 "Proceedings from the Conference on Disaster Preparedness - The Place of Earthquake Education in Our Schools," Edited by K.E.K. Ross, 12/31/89, (PB90-207895).

NCEER-89-0018 "Multidimensional Models of Hysteretic Material Behavior for Vibration Analysis of Shape Memory Energy Absorbing Devices, by E.J. Graesser and F.A. Cozzarelli, 6/7/89, (PB90-164146/AS).

NCEER-89-0019 "Nonlinear Dynamic Analysis of Three-Dimensional Base Isolated Structures (3D-BASIS)," by S. Nagarajaiah, A.M. Reinhorn and M.C. Constantinou, 8/3/89, (PB90-161936/AS).

NCEER-89-0020 "Structural Control Considering Time-Rate of Control Forces and Control Rate Constraints," by F.Y. Cheng and C.P. Pantelides, 8/3/89, (PB90-120445/AS).

NCEER-89-0021 "Subsurface Conditions of Memphis and Shelby County," by K.W. Ng, T-S. Chang and H-H.M. Hwang, 7/26/89, (PB90-120437/AS).

NCEER-89-0022 "Seismic Wave Propagation Effects on Straight Jointed Buried Pipelines," by K. Elhmadi and M.J. O'Rourke, 8/24/89, (PB90-162322/AS).

NCEER-89-0023 "Workshop on Serviceability Analysis of Water Delivery Systems," edited by M. Grigoriu, 3/6/89, (PB90-127424/AS).

NCEER-89-0024 "Shaking Table Study of a 1/5 Scale Steel Frame Composed of Tapered Members," by K.C. Chang, J.S. Hwang and G.C. Lee, 9/18/89, (PB90-160169/AS).

NCEER-89-0025 "DYNA1D: A Computer Program for Nonlinear Seismic Site Response Analysis - Technical Documentation," by Jean H. Prevost, 9/14/89, (PB90-161944/AS).

NCEER-89-0026 "1:4 Scale Model Studies of Active Tendon Systems and Active Mass Dampers for Aseismic Protection," by A.M. Reinhorn, T.T. Soong, R.C. Lin, Y.P. Yang, Y. Fukao, H. Abe and M. Nakai, 9/15/89, (PB90-173246/AS).

NCEER-89-0027 "Scattering of Waves by Inclusions in a Nonhomogeneous Elastic Half Space Solved by Boundary Element Methods," by P.K. Hadley, A. Askar and A.S. Cakmak, 6/15/89, (PB90-145699/AS).

NCEER-89-0028 "Statistical Evaluation of Deflection Amplification Factors for Reinforced Concrete Structures," by H.H.M. Hwang, J-W. Jaw and A.L. Ch'ng, 8/31/89, (PB90-164633/AS).

NCEER-89-0029 "Bedrock Accelerations in Memphis Area Due to Large New Madrid Earthquakes," by H.H.M. Hwang, C.H.S. Chen and G. Yu, 11/7/89, (PB90-162330/AS).

NCEER-89-0030 "Seismic Behavior and Response Sensitivity of Secondary Structural Systems," by Y.Q. Chen and T.T. Soong, 10/23/89, (PB90-164658/AS).

NCEER-89-0031 "Random Vibration and Reliability Analysis of Primary-Secondary Structural Systems," by Y. Ibrahim, M. Grigoriu and T.T. Soong, 11/10/89, (PB90-161951/AS).

NCEER-89-0032 "Proceedings from the Second U.S. - Japan Workshop on Liquefaction, Large Ground Deformation and Their Effects on Lifelines, September 26-29, 1989," Edited by T.D. O'Rourke and M. Hamada, 12/1/89, (PB90-209388/AS).

NCEER-89-0033 "Deterministic Model for Seismic Damage Evaluation of Reinforced Concrete Structures," by J.M. Bracci, A.M. Reinhorn, J.B. Mander and S.K. Kunnath, 9/27/89.

NCEER-89-0034 "On the Relation Between Local and Global Damage Indices," by E. DiPasquale and A.S. Cakmak, 8/15/89, (PB90-173865).

NCEER-89-0035 "Cyclic Undrained Behavior of Nonplastic and Low Plasticity Silts," by A.J. Walker and H.E. Stewart, 7/26/89, (PB90-183518/AS).

NCEER-89-0036 "Liquefaction Potential of Surficial Deposits in the City of Buffalo, New York," by M. Budhu, R. Giese and L. Baumgrass, 1/17/89, (PB90-208455/AS).

NCEER-89-0037 "A Determinstic Assessment of Effects of Ground Motion Incoherence," by A.S. Veletsos and Y. Tang, 7/15/89, (PB90-164294/AS).

NCEER-89-0038 "Workshop on Ground Motion Parameters for Seismic Hazard Mapping," July 17-18, 1989, edited by R.V. Whitman, 12/1/89, (PB90-173923/AS).

NCEER-89-0039 "Seismic Effects on Elevated Transit Lines of the New York City Transit Authority," by C.J. Costantino, C.A. Miller and E. Heymsfield, 12/26/89, (PB90-207887/AS).

NCEER-89-0040 "Centrifugal Modeling of Dynamic Soil-Structure Interaction," by K. Weissman, Supervised by J.H. Prevost, 5/10/89, (PB90-207879/AS).

NCEER-89-0041 "Linearized Identification of Buildings With Cores for Seismic Vulnerability Assessment," by I-K. Ho and A.E. Aktan, 11/1/89, (PB90-251943/AS).

NCEER-90-0001 "Geotechnical and Lifeline Aspects of the October 17, 1989 Loma Prieta Earthquake in San Francisco," by T.D. O'Rourke, H.E. Stewart, F.T. Blackburn and T.S. Dickerman, 1/90, (PB90-208596/AS).

NCEER-90-0002 "Nonnormal Secondary Response Due to Yielding in a Primary Structure," by D.C.K. Chen and L.D. Lutes, 2/28/90, (PB90-251976/AS).

NCEER-90-0003 "Earthquake Education Materials for Grades K-12," by K.E.K. Ross, 4/16/90, (PB91-113415/AS).

NCEER-90-0004 "Catalog of Strong Motion Stations in Eastern North America," by R.W. Busby, 4/3/90, (PB90-251984)/AS.

NCEER-90-0005 "NCEER Strong-Motion Data Base: A User Manuel for the GeoBase Release (Version 1.0 for the Sun3)," by P. Friberg and K. Jacob, 3/31/90 (PB90-258062/AS).

NCEER-90-0006 "Seismic Hazard Along a Crude Oil Pipeline in the Event of an 1811-1812 Type New Madrid Earthquake," by H.H.M. Hwang and C-H.S. Chen, 4/16/90(PB90-258054).

NCEER-90-0007 "Site-Specific Response Spectra for Memphis Sheahan Pumping Station," by H.H.M. Hwang and C.S. Lee, 5/15/90, (PB91-108811/AS).

NCEER-90-0008 "Pilot Study on Seismic Vulnerability of Crude Oil Transmission Systems," by T. Ariman, R. Dobry, M. Grigoriu, F. Kozin, M. O'Rourke, T. O'Rourke and M. Shinozuka, 5/25/90, (PB91-108837/AS).

NCEER-90-0009 "A Program to Generate Site Dependent Time Histories: EQGEN," by G.W. Ellis, M. Srinivasan and A.S. Cakmak, 1/30/90, (PB91-108829/AS).

NCEER-90-0010 "Active Isolation for Seismic Protection of Operating Rooms," by M.E. Talbott, Supervised by M. Shinozuka, 6/8/9, (PB91-110205/AS).

NCEER-90-0011 "Program LINEARID for Identification of Linear Structural Dynamic Systems," by C-B. Yun and M. Shinozuka, 6/25/90, (PB91-110312/AS).

NCEER-90-0012 "Two-Dimensional Two-Phase Elasto-Plastic Seismic Response of Earth Dams," by A.N. Yiagos, Supervised by J.H. Prevost, 6/20/90, (PB91-110197/AS).

NCEER-90-0013 "Secondary Systems in Base-Isolated Structures: Experimental Investigation, Stochastic Response and Stochastic Sensitivity," by G.D. Manolis, G. Juhn, M.C. Constantinou and A.M. Reinhorn, 7/1/90, (PB91-110320/AS).

NCEER-90-0014 "Seismic Behavior of Lightly-Reinforced Concrete Column and Beam-Column Joint Details," by S.P. Pessiki, C.H. Conley, P. Gergely and R.N. White, 8/22/90, (PB91-108795/AS).

NCEER-90-0015 "Two Hybrid Control Systems for Building Structures Under Strong Earthquakes," by J.N. Yang and A. Danielians, 6/29/90, (PB91-125393/AS).

NCEER-90-0016 "Instantaneous Optimal Control with Acceleration and Velocity Feedback," by J.N. Yang and Z. Li, 6/29/90, (PB91-125401/AS).

NCEER-90-0017 "Reconnaissance Report on the Northern Iran Earthquake of June 21, 1990," by M. Mehrain, 10/4/90, (PB91-125377/AS).

NCEER-90-0018 "Evaluation of Liquefaction Potential in Memphis and Shelby County," by T.S. Chang, P.S. Tang, C.S. Lee and H. Hwang, 8/10/90, (PB91-125427/AS).

NCEER-90-0019 "Experimental and Analytical Study of a Combined Sliding Disc Bearing and Helical Steel Spring Isolation System," by M.C. Constantinou, A.S. Mokha and A.M. Reinhorn, 10/4/90, (PB91-125385/AS).

NCEER-90-0020 "Experimental Study and Analytical Prediction of Earthquake Response of a Sliding Isolation System with a Spherical Surface," by A.S. Mokha, M.C. Constantinou and A.M. Reinhorn, 10/11/90, (PB91-125419/AS).

NCEER-90-0021 "Dynamic Interaction Factors for Floating Pile Groups," by G. Gazetas, K. Fan, A. Kaynia and E. Kausel, 9/10/90, (PB91-170381/AS).

NCEER-90-0022 "Evaluation of Seismic Damage Indices for Reinforced Concrete Structures," by S. Rodríguez-Gómez and A.S. Cakmak, 9/30/90, PB91-171322/AS).

NCEER-90-0023 "Study of Site Response at a Selected Memphis Site," by H. Desai, S. Ahmad, E.S. Gazetas and M.R. Oh, 10/11/90, (PB91-196857/AS).

NCEER-90-0024 "A User's Guide to Strongmo: Version 1.0 of NCEER's Strong-Motion Data Access Tool for PCs and Terminals," by P.A. Friberg and C.A.T. Susch, 11/15/90, (PB91-171272/AS).

NCEER-90-0025 "A Three-Dimensional Analytical Study of Spatial Variability of Seismic Ground Motions," by L-L. Hong and A.H.-S. Ang, 10/30/90, (PB91-170399/AS).

NCEER-90-0026 "MUMOID User's Guide - A Program for the Identification of Modal Parameters," by S. Rodríguez-Gómez and E. DiPasquale, 9/30/90, (PB91-171298/AS).

NCEER-90-0027 "SARCF-II User's Guide - Seismic Analysis of Reinforced Concrete Frames," by S. Rodríguez-Gómez, Y.S. Chung and C. Meyer, 9/30/90, (PB91-171280/AS).

NCEER-90-0028 "Viscous Dampers: Testing, Modeling and Application in Vibration and Seismic Isolation," by N. Makris and M.C. Constantinou, 12/20/90 (PB91-190561/AS).

NCEER-90-0029 "Soil Effects on Earthquake Ground Motions in the Memphis Area," by H. Hwang, C.S. Lee, K.W. Ng and T.S. Chang, 8/2/90, (PB91-190751/AS).

NCEER-91-0001 "Proceedings from the Third Japan-U.S. Workshop on Earthquake Resistant Design of Lifeline Facilities and Countermeasures for Soil Liquefaction, December 17-19, 1990," edited by T.D. O'Rourke and M. Hamada, 2/1/91, (PB91-179259/AS).

NCEER-91-0002 "Physical Space Solutions of Non-Proportionally Damped Systems," by M. Tong, Z. Liang and G.C. Lee, 1/15/91, (PB91-179242/AS).

NCEER-91-0003 "Kinematic Seismic Response of Single Piles and Pile Groups," by K. Fan, G. Gazetas, A. Kaynia, E. Kausel and S. Ahmad, 1/10/91, to be published.

NCEER-91-0004 "Theory of Complex Damping," by Z. Liang and G. Lee, to be published.

NCEER-91-0005 "3D-BASIS - Nonlinear Dynamic Analysis of Three Dimensional Base Isolated Structures: Part II," by S. Nagarajaiah, A.M. Reinhorn and M.C. Constantinou, 2/28/91, (PB91-190553/AS).

NCEER-91-0006 "A Multidimensional Hysteretic Model for Plasticity Deforming Metals in Energy Absorbing Devices," by E.J. Graesser and F.A. Cozzarelli, 4/9/91.

NCEER-91-0007 "A Framework for Customizable Knowledge-Based Expert Systems with an Application to a KBES for Evaluating the Seismic Resistance of Existing Buildings," by E.G. Ibarra-Anaya and S.J. Fenves, 4/9/91, (PB91-210930/AS).

NCEER-91-0008 "Nonlinear Analysis of Steel Frames with Semi-Rigid Connections Using the Capacity Spectrum Method," by G.G. Deierlein, S-H. Hsieh, Y-J. Shen and J.F. Abel, 7/2/91.

NCEER-91-0009 "Earthquake Education Materials for Grades K-12," by K.E.K. Ross, 4/30/91, (PB91-212142/AS).

NCEER-91-0010 "Phase Wave Velocities and Displacement Phase Differences in a Harmonically Oscillating Pile," by N. Makris and G. Gazetas, 7/8/91, (PB92-108356/AS).

NCEER-91-0011 "Dynamic Characteristics of a Full-Sized Five-Story Steel Structure and a 2/5 Model," by K.C. Chang, G.C. Yao, G.C. Lee, D.S. Hao and Y.C. Yeh," to be published.

NCEER-91-0012 "Seismic Response of a 2/5 Scale Steel Structure with Added Viscoelastic Dampers," by K.C. Chang, T.T. Soong, S-T. Oh and M.L. Lai, 5/17/91 (PB92-110816/AS).

NCEER-91-0013 "Earthquake Response of Retaining Walls; Full-Scale Testing and Computational Modeling," by S. Alampalli and A-W.M. Elgamal, 6/20/91, to be published.

NCEER-91-0014 "3D-BASIS-M: Nonlinear Dynamic Analysis of Multiple Building Base Isolated Structures," by P.C. Tsopelas, S. Nagarajaiah, M.C. Constantinou and A.M. Reinhorn, 5/28/91.

NCEER-91-0015 "Evaluation of SEAOC Design Requirements for Sliding Isolated Structures," by D. Theodossiou and M.C. Constantinou, 6/10/91.

NCEER-91-0016 "Closed-Loop Modal Testing of a 27-Story Reinforced Concrete Flat Plate-Core Building," by H.R. Somaprasad, T. Toksoy, H. Yoshiyuki and A.E. Aktan, 7/15/91.

NCEER-91-0017 "Shake Table Test of a 1/6 Scale Two-Story Lightly Reinforced Concrete Building," by A.G. El-Attar, R.N. White and P. Gergely, 2/28/91, to be published.

NCEER-91-0018 "Shake Table Test of a 1/8 Scale Three-Story Lightly Reinforced Concrete Building," by A.G. El-Attar, R.N. White and P. Gergely, 2/28/91, to be published.

NCEER-91-0019 "Transfer Functions for Rigid Rectangular Foundations," by A.S. Veletsos, A.M. Prasad and W.H. Wu, 7/31/91, to be published.

NCEER-91-0020 "Hybrid Control of Seismic-Excited Nonlinear and Inelastic Structural Systems," by J.N. Yang, Z. Li and A. Danielians, 8/1/91.

NCEER-91-0021 "The NCEER-91 Earthquake Catalog: Improved Intensity-Based Magnitudes and Recurrence Relations for U.S. Earthquakes East of New Madrid," by L. Seeber and J.G. Armbruster, 8/28/91, to be published.

NCEER-91-0022 "Proceedings from the Implementation of Earthquake Planning and Education in Schools: The Need for Change - The Roles of the Changemakers," by K.E.K. Ross and F. Winslow, 7/23/91.

NCEER-91-0023 "A Study of Reliability-Based Criteria for Seismic Design of Reinforced Concrete Frame Buildings," by H.H.M. Hwang and H-M. Hsu, 8/10/91.

NCEER-91-0024 "Experimental Verification of a Number of Structural System Identification Algorithms," by R.G. Ghanem, H. Gavin and M. Shinozuka, 9/18/91.

NCEER-91-0025 "Probabilistic Evaluation of Liquefaction Potential," by H.H.M. Hwang and C.S. Lee," 11/25/91.

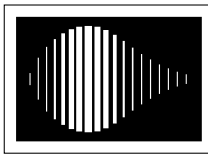

NATIONAL CENTER FOR EARTHQUAKE ENGINEERING RESEARCH

Headquartered at the State University of New York at Buffalo

State University of New York at Buffalo
Red Jacket Quadrangle
Buffalo, New York 14261
Telephone: 716/645-3391
FAX: 716/645-3399

ISSN 1088-3800